E 64

AEC Category: PHYSICS

CEX-58.9

CIVIL EFFECTS STUDY

A MODEL DESIGNED TO PREDICT THE MOTION OF OBJECTS TRANSLATED BY CLASSICAL BLAST WAVES

I. Gerald Bowen, Ray W. Albright,
E. Royce Fletcher, and Clayton S. White

Issuance Date: June 29, 1961

CIVIL EFFECTS TEST OPERATIONS
U.S. ATOMIC ENERGY COMMISSION

NOTICE

This report is published in the interest of providing information which may prove of value to the reader in his study of effects data derived principally from nuclear weapons tests.

This document is based on information available at the time of preparation which may have subsequently been expanded and re-evaluated. Also, in preparing this report for publication, some classified material may have been removed. Users are cautioned to avoid interpretations and conclusions based on unknown or incomplete data.

PRINTED IN USA
Price $1.25. Available from the Office of
Technical Services, Department of Commerce,
Washington 25, D. C.

USAEC Office of Technical Information Extension
Oak Ridge, Tennessee

A MODEL DESIGNED TO PREDICT THE MOTION OF OBJECTS TRANSLATED BY CLASSICAL BLAST WAVES

By

I. Gerald Bowen, Ray W. Albright,
E. Royce Fletcher, and Clayton S. White

Approved by: R. L. CORSBIE
Director
Civil Effects Test Operations

Lovelace Foundation for Medical Education and Research
Albuquerque, New Mexico
January 1961

ABSTRACT

A theoretical model was developed for the purpose of predicting the motion of objects translated by winds associated with "classical" blast waves produced by explosions. Among the factors omitted from the model for the sake of simplicity were gravity and the friction that may occur between the displaced object and the surface upon which it initially rested. Numerical solutions were obtained (up to the time when maximum missile velocity occurs) in terms of dimensionless quantities to facilitate application to specific blast situations. The results were computed within arbitrarily chosen limits for blast waves with shock strengths from 0.068 to 1.7 atm (1 to 25 psi at sea level) for displaced objects with aerodynamic characteristics ranging from those of a human being to those of 10-mg stones and for weapon yields at least as small as 1 kt or as large as 20 Mt.

ACKNOWLEDGMENTS

The authors wish to acknowledge helpful discussions with Sandia Corporation personnel in the Weapons Effects Department, especially in regard to the physics of the blast wave. Among those giving consultation were Mr. L. J. Vortman, Dr. M. L. Merritt, Dr. T. B. Cook, and Dr. C. D. Broyles.

Particular appreciation is expressed to Dr. Harold L. Brode of Rand Corporation for the blast-wave data that he supplied to us in the form of empirical equations derived from results computed from a point-source explosion model.

Computations necessary for the numerical solution of the equations of motion derived in this report were made possible through the cooperation of the Systems Analysis Department of Sandia Corporation. This department not only made available to us an electronic digital computer but also assisted in the preparation of a suitable program to accomplish the necessary computations. For this help we wish to thank Dr. W. W. Bledsoe, Dr. D. R. Morrison, Mrs. Pauline Van Delinder, and Mr. W. W. Whisler.

Also, appreciation is expressed to Lovelace Foundation personnel who assisted in the preparation of this report: Mr. Jerome Kleinfeld, Mr. Malcolm A. Osoff, and Mr. David W. Roeder for preparation of data for charts and tables; Mr. Robert A. Smith, Mr. Roy D. Caton, and Mr. George S. Bevil for preparation of illustrative material; Mrs. Isabell D. Benton, Mrs. Martina B. Smith, Mrs. Joanna Upthegrove, and Mrs. Frances E. Moore for editorial and secretarial assistance in preparation of the manuscript.

Lastly, the work reported here is a segment of that carried out on the biological effects of blast from bombs made possible through support by the Division of Biology and Medicine of the Atomic Energy Commission under contract with the Lovelace Foundation. The interest and encouragement of Dr. C. L. Dunham, Mr. R. L. Corsbie, Dr. H. D. Bruner, and Dr. J. F. Bonner, all of the Atomic Energy Commission, are gratefully acknowledged.

CONTENTS

CONTENTS (Continued)

ILLUSTRATIONS

ILLUSTRATIONS (Continued)

TABLES

Chapter 1

INTRODUCTION

1.1 OBJECTIVES

During the 1955 and 1957 Test Operations at the Nevada Test Site, the masses and velocities of over 20,000 objects (window-glass fragments, stones, spheres, sticks, etc.) which were translated by nuclear-produced blast waves were experimentally determined,[1-4] along with a time-displacement history of an anthropometric dummy simulating man.[5] The availability of such a mass of data stimulated an analytical study calculated to arrive at a mathematical formulation capable of predicting the translation of objects by blast, particularly since this data offered an empirical fabric against which to test the success of the analytical effort.

The purpose of this report is to describe, step by step, the theoretical studies that have resulted in a mathematical model capable of predicting the motion of objects utilizing selected basic blast parameters. This model, however, is applicable only to those situations in which *classical wave forms exist.

1.2 SCOPE AND LIMITATIONS

The applicability of the model itself has no well-defined limits; however, the numerical solutions that were obtained and are reported herein have been arbitrarily limited in scope. In general, the aim was to compute velocity, displacement, and acceleration as a function of time for objects ranging in size from a pea to man; these computations were to cover blast waves with shock overpressures from 1 to 25 psi (14.7-psi ambient pressure) and weapon yields from 1 kt to 20 Mt.

Another class of limitations is invoked not by the scope of the computations, but by the model itself. Formulation of a workable model was facilitated by the use of certain simplifying assumptions. These assumptions, which are discussed below, have not, in general, caused serious discrepancies between predicted velocities and those measured in the field operations, particularly in those situations where the blast wave was classical.†

As a practical approach, it was assumed first that the effect of surface friction was negligible. It has been observed that fairly large objects tend to be lofted when subjected to blast waves; the more intense the blast, the heavier the object that it is capable of lifting against gravity. Nonspherical objects could develop either positive or negative lift depending on their orientation to the wind. Thus, the validity of the no-friction assumption is dependent upon the strength of the blast wave, the object under consideration, its random orientation, and the nature of the surface over which translation occurs. It will be shown later that certain uses can be made of the data even for situations in which surface friction is a significant factor.

---

*The term "classical blast wave" is used in this report to mean the typical wave not appreciably modified by terrain effects and possessing a well-defined shock front.

†A limited discussion of the agreement between predicted and measured velocities is made later in this report. A more complete treatment will be found in Ref. 3.

A second approximation made concerned the assumption that there was no gain or loss of energy as a result of the object's moving with or against gravity. The kinetic energy that is lost during lofting would be regained as the object fell to its original elevation, thus mitigating somewhat the error in the predicted motion.

Third, only the propelling force of the wind was considered. Another force that might have been included was that due to differences in overpressure between one side of the object and the other during passage of the shock front (diffractive loading). Since the bodies being considered were relatively small (up to the size of man), the classical blast wave would engulf the object very quickly and impart only a small momentum as a result of the overpressure itself.

Fourth, it was assumed that there was no change in the properties of an object which governed acceleration (area presented to the wind, drag coefficient, and mass) during the accelerative phase of displacement. For irregular, rigid objects that are nearly spherical, such as stones, this is a reasonable assumption. For objects that are obviously nonspherical or deformable, prediction of a range of velocities taking into account both maximum and minimum drag areas is often used. Another useful procedure is to employ the average drag area derived from the concept of random orientation.[6]

Fifth, no allowance was made for the fact that a displaced object may be moved to a lower overpressure region and thus be acted upon by correspondingly weaker blast winds. The results of the computations themselves seem to justify the neglection of this phenomenon. It will be shown that displaced objects receive a large percentage of their velocities in a relatively short distance over which the decay of the blast wave is small.

REFERENCES

1. I. Gerald Bowen, Allen F. Strehler, and Mead B. Wetherbe, Distribution and Density of Missiles from Nuclear Explosions, Operation Teapot Report, WT-1168, March 1956.
2. I. Gerald Bowen, Donald R. Richmond, Mead B. Wetherbe, and Clayton S. White, Biological Effects of Blast from Bombs. Glass Fragments as Penetrating Missiles and Some of the Biological Implications of Glass Fragmented by Atomic Explosions, Report AECU-3350, June 18, 1956.
3. I. Gerald Bowen et al., Secondary Missiles Generated by Nuclear-produced Blast Waves, Operation Plumbbob Report, WT-1468 (in preparation).
4. V. C. Goldizen, D. R. Richmond, and T. L. Chiffelle, Missile Studies with a Biological Target, Operation Plumbbob Report, WT-1470, January 1961.
5. R. V. Taborelli, I. G. Bowen, and E. R. Fletcher, Tertiary Effects of Blast–Displacement, Operation Plumbbob Report, WT-1469, May 22, 1959.
6. E. Royce Fletcher et al., Determination of Aerodynamic Drag Parameters of Small Irregular Objects by Means of Drop Tests, Civil Effects Test Operations, Report CEX-59.14 (in preparation).

Chapter 2

ANALYTICAL PROCEDURE

2.1 NOMENCLATURE

The terminology used in this study is defined in this section. A lower-case letter is used to represent a quantity with dimensions. In general, the same letter is capitalized if the quantity is made dimensionless by an appropriate factor or factors. Thus, the dimensionless term is represented by its principle variable. The factors, or parameters, used to make quantities dimensionless invariably are constants for any given blast situation.

α = acceleration coefficient = sC_d/m
$A = \alpha p_0 t_u^+/c_0$
c_0 = speed of sound in undisturbed air
C_d = drag coefficient of moving object
d = distance of travel of moving object
d_m = distance of travel of moving object when maximum velocity is reached
$D = d/(t_u^+ c_0)$
I = overpressure impulse = $\int_0^{t_p^+} P\,dt$
m = mass of moving object
p = overpressure or pressure in excess of p_0
p_0 = pressure of undisturbed air
p_s = maximum or shock overpressure
$P = p/p_0$
$P_s = p_s/p_0$, shock overpressure in atmospheres
q = dynamic pressure = $(1/2)\rho u^2$
q_s = dynamic pressure at the shock front
$Q = q/p_0$
$Q_s = q_s/p_0$
ρ = air density
s = area presented to wind by moving object
t = time after arrival of blast wave
t_p^+ = duration of positive pressure phase of blast wave
t_u^+ = duration of winds in the direction of propagation of the blast wave
$T = t/t_p^+$
u = velocity of the air
$U = u/c_0$
v = velocity of the moving object
v_m = maximum velocity of moving object
$V = v/c_0$
$\dot{v}$ = acceleration of moving object
$\dot{V} = \dot{v}t_u^+/c_0$
W = weapon yield in kilotons
$\dot{x}$ = velocity of propagation of the pressure disturbance

$\dot{X} = \dot{x}/c_0$
$Z = t/t_u^+$

NOTE: Any variable that is underlined indicates the average value taken over a particular time interval.

2.2 EQUATIONS OF MOTION

2.2.1 Fundamental Concepts

Newton's second law of motion can be stated as

$$\text{Force} = m\frac{dv}{dt}$$

and the drag force on a moving object is

$$\text{Force} = \frac{1}{2}\rho(u - v)^2\, sC_d$$

since the net wind moving past the object is $(u - v)$. Combining the above equations and solving for dv, we obtain

$$dv = \rho\frac{(u - v)^2}{2}\frac{sC_d}{m}dt \tag{2.1}$$

It was convenient to isolate and label the physical parameters that involve the moving object in Eq. 2.1.

$$\frac{sC_d}{m} = \alpha \tag{2.2}$$

Now, α can be called "acceleration coefficient" since it completely describes the object in so far as the computation of velocity vs. time is concerned. Thus, two objects possessing the same value of α, regardless of dissimilarity of shape, size, and mass, would experience the same increase in velocity if exposed to the same or similar blast waves.

2.2.2 Time Correction

Since the moving object, or missile, travels along with the blast wave, the time during which it is exposed to blast winds is longer the higher its velocity is in relation to the velocity of propagation of the pressure disturbance and associated winds. Consider a small segment of the blast wave of length dx where the air-particle density and velocity are approximately constant. If this segment moves with a velocity $\dot{x}$, then

$$dx = \dot{x}\, dt$$

where dt is the time required for the segment dx to pass a fixed point. Similarly, the velocity of propagation of a blast-wave segment past a missile that itself is moving at velocity v is $(\dot{x} - v)$, and

$$dx = (\dot{x} - v)\, dt'$$

where dt′ is the time required for the blast segment to pass the missile. By eliminating dx between the above equations, we obtain

$$dt' = dt\frac{\dot{x}}{\dot{x} - v} \tag{2.3}$$

Combining Eqs. 2.1 and 2.2 and substituting the corrected time dt′ of Eq. 2.3 for dt, we obtain

$$dv = \frac{1}{2}\rho\alpha(u - v)^2 \frac{\dot{x}}{(\dot{x} - v)} dt \tag{2.4}$$

It was more convenient to work with dynamic pressure, $q = (1/2)\rho u^2$, than with air density. For this reason Eq. 2.4 was modified to

$$dv = q\alpha\left(\frac{u - v}{u}\right)^2 \frac{\dot{x}}{(\dot{x} - v)} dt \tag{2.5}$$

2.2.3 Dimensional Analysis

The blast-wave variables in Eq. 2.5 are determined as a function of time by four parameters: (1) shock overpressure, p_s; (2) ambient pressure, p_0; (3) duration of the positive winds, t_u^+; and (4) speed of sound in the undisturbed air, c_0. Computations were made for particular values of shock overpressure in atmospheres, $P_s = p_s/p_0$. The last three parameters, however, were used to make the variables in Eq. 2.5 dimensionless. The obvious advantage of this procedure is that computed values of missile velocity, distance of travel, and acceleration can be modified after the computations have been made to fit any blast situation defined by p_0, t_u^+, and c_0.

The variables of Eq. 2.5 were made dimensionless through the application of the following algebraic operations: (1) both sides of the equation were divided by c_0, (2) the numerators and the denominators of the two fractions were divided by c_0, (3) α was multiplied by p_0 and q was divided by p_0, and (4) t was divided by t_u^+ and α was multiplied by t_u^+.

After these operations have been performed, Eq. 2.5 becomes

$$d\left(\frac{v}{c_0}\right) = \left(\frac{q}{p_0}\right)\left(\frac{\alpha p_0 t_u^+}{c_0}\right)\left[\frac{(u/c_0) - (v/c_0)}{u/c_0}\right]^2\left[\frac{\dot{x}/c_0}{(\dot{x}/c_0) - (v/c_0)}\right] d\left(\frac{t}{t_u^+}\right) \tag{2.6}$$

and, after appropriate substitutions (see Sec. 2.1, Nomenclature)

$$dV = QA\left(\frac{U - V}{U}\right)^2 \frac{\dot{X}}{\dot{X} - V} dZ \tag{2.7}$$

Two additional quantities are used in dimensionless form, distance of travel and acceleration. Since both are functions of velocity and time, their dimensionless forms are determined by dimensionless velocity and time. Thus

$$D = VZ = \frac{v}{c_0}\frac{t}{t_u^+} = \frac{d}{c_0 t_u^+} \tag{2.8}$$

and

$$\dot{V} = \frac{V}{Z} = \frac{v t_u^+}{c_0 t} = \frac{\dot{v} t_u^+}{c_0} \tag{2.9}$$

2.2.4 Approximation Solution

The explicit expressions of Q, U, and $\dot{X}$ as a function of time for a particular blast wave are very cumbersome. Added to this difficulty is the fact that the variable V cannot be separated from the time-dependent variables (see Eq. 2.7). Hope for a complete mathematical solution was soon abandoned.

A stepwise solution was then attempted which would permit the blast parameters to be held constant for small increments of time but would allow the missile velocity to vary as a nonlinear function of time. So that a simple mathematical integration can be accomplished, the

time-correction term, $\dot{X}/(\dot{X} - V)$, was not included. Thus

$$\int_{V_0}^{V_0+\Delta V} \frac{dV}{(\underline{U} - V)^2} = \underline{Q}A \int_{Z_0}^{Z_0+\Delta Z'} dZ \qquad (2.10)$$

where V_0 and Z_0 are the velocity and time, respectively, at the beginning of the time period and ΔV is the change in velocity in time $\Delta Z'$. Underlined U and Q indicate average values over the time $\Delta Z'$.

Integration of Eq. 2.10 and substitution of limits yields

$$\frac{1}{\underline{U} - V_0 - \Delta V} - \frac{1}{\underline{U} - V_0} = \underline{Q}A\ \Delta Z' \qquad (2.11)$$

The average missile velocity during the time period $\Delta Z'$ is $[V_0 + (1/2)\Delta V]$. Thus the time-correction term (see Eq. 2.3) expressed in dimensionless incremental form is

$$\Delta Z' = \Delta Z \frac{\underline{\dot{X}}}{\underline{\dot{X}} - V_0 - (1/2)\Delta V} \qquad (2.12)$$

Eliminating $\Delta Z'$ between Eqs. 2.11 and 2.12 and solving for ΔV, the following is obtained

$$\Delta V = e + f - \sqrt{e^2 + 2fg + f^2} \qquad (2.13)$$

where $e = \underline{\dot{X}} - V_0$

$f = \underline{AQ}\ (\underline{U} - V_0)\underline{\dot{X}}\ (\Delta Z/\underline{U}^2)$

$g = \underline{\dot{X}} - \underline{U}$

The velocity at the end of any step is the summation of the ΔV's computed from the beginning of the integration.

Incremental distance, ΔD, was computed by the following:

$$\Delta D = [V_0 + (1/2)\Delta V]\ \Delta Z' \qquad (2.14)$$

where V_0 refers to the velocity at the beginning of the step. $\Delta Z'$ is defined in Eq. 2.12.

Evaluation of acceleration ($\dot{V} = dV/dZ$) presented little difficulty since integration was not involved. Furthermore, the time-correction term was not necessary because, by definition, $\dot{V}$ is the instantaneous time rate of change in velocity. Thus, the following equation was formed from Eq. 2.7:

$$\dot{V} = \frac{dV}{dZ} = QA\left(\frac{U - V}{U}\right)^2 \qquad (2.15)$$

2.3 EVALUATION OF BLAST-WAVE VARIABLES

2.3.1 General Remarks

A particular classical blast wave can be completely defined mathematically by the parameters of shock strength (p_s/p_0), duration, and either the velocity of sound or the temperature for ambient conditions. Secondary-missile computations were made for selected values of shock strength, each of which is applicable to any value of duration (and thus bomb yield) or ambient sound velocity between wide limits.

2.3.2 Dynamic Pressure and Wind Velocity

Although dynamic pressure (from which wind may be computed) has been measured in ac-

tual blast situations, values computed from theoretical considerations were used in this study. The reason for this was both the higher reliability and the greater facility for numerical treatment of the computed parameters over the measured ones. Of the several studies made of the blast wave, those made by Harold L. Brode of Rand Corporation[1,2] were found to be most useful for the present study. The equations[3] listed below are empirical relations determined by fitting curves to computed blast data. In terminology consistent with the present study, dynamic pressure as a function at shock overpressure and time is given by

$$Q = Q_S\ (1 - Z)\ [Je^{-\gamma Z} + Ke^{-\delta Z}] \tag{2.16}$$

where $Q_S = \left(\dfrac{2.5\ P_S^2}{7 + P_S}\right)\left(\dfrac{1 + 2 \times 10^{-8}\ P_S^4}{1 + 10^{-8}\ P_S^4}\right)$

$J = 1.186\ P_S^{1/3}$ for $P_S < 0.6$

$J = 1$ for $0.6 \leq P_S \leq 1.0$

$J = (10^4\ P_S^{-1/4})/(10^4 + P_S^2)$ for $P_S > 1$

$K = 1 - J$

$\gamma = (1/4) + 3.6\ P_S^{1/2}$

$\delta = (7 + 8\ P_S^{1/2}) + 2\ P_S^2/(240 + P_S)$

The relation for wind, or particle, velocity is

$$U = U_S\ (1 - Z)\ e^{-\nu Z} \tag{2.17}$$

where $U_S = (P_S)/(1 + P_S^{1/2})$

$\nu = P_S^{1/3} + 0.0032\ P_S^{3/2}$

$D = \int_0^Z U\, dZ = \dfrac{U_S\,(e^{-\nu} + \nu - 1)}{\nu^2}$

2.3.3 Overpressure vs. Time and Overpressure Impulse

Overpressure as a function of time does not enter directly into the computation of secondary-missile behavior; nevertheless, it seems appropriate to consider this relation since it is the most commonly measured parameter of the real blast wave. Thus, overpressure-time can be considered to be the bridge between secondary-missile field data and the computed data resulting from the present study.

The following overpressure-time relation was obtained from Brode:[1-3]

$$P = P_s\ (1 - T)\ (ae^{-iT} + be^{-jT}) \tag{2.18}$$

where $a = \dfrac{2.282\ (8 + P_S)}{27.658 + P_S + 1.2\ P_S^2 + 0.007\ P_S^3} + 0.23$

$b = 1 - a$

$i = \sqrt{\dfrac{P_S}{1 + 0.1\ P_S}} + \dfrac{1.5\ P_S^2}{1500 + P_S^{3/2}}$

$j = 9 + 1.4\ P_S$

Pressure instrumentation used in field work often produces a more accurate measurement of overpressure impulse than of shock overpressure. Indeed, an improved estimate of shock overpressure can be made by making use of the impulse relation described below.

Overpressure impulse is defined as

$$I = \int_0^{t_p^+} P\ dt \tag{2.19}$$

However, to facilitate integration of Eq. 2.18 in terms of normalized time, the following relation was used:

$$T = t/t_p^+ \tag{2.20}$$

thus,

$$dt = t_p^+ \, dT \tag{2.21}$$

A combination of Eqs. 2.19 and 2.21 gives

$$I = t_p^+ \int_0^1 P \, dT \tag{2.22}$$

Integration of Eq. 2.18 in the manner indicated by Eq. 2.22 yields the following:

$$I = P_s t_p^+ \left[\frac{a}{\underset{i}{\cancel{e}}^2} (e^{-i} + i - 1) + \frac{b}{\underset{j}{\cancel{k}}^2} (e^{-j} + j - 1) \right] \tag{2.23}$$

Figure 2.1, a plot of P_s in atmospheres as a function of I/t_p^+ also in atmospheres, illustrates this relation graphically. This plot can be thought of as defining the "shape factor" of the overpressure-time curve as a function of maximum overpressure. If impulse, I, and duration, t_p^+, are measured by suitable instrumentation, then a value of shock overpressure can be determined from the curve shown in this figure.

2.3.4 Duration Concepts

(a) *Positive-overpressure Duration.* To evaluate the computed motion parameters for a particular yield, it is obviously necessary to know the duration of the blast wave (identified by peak or shock overpressure) of interest. For this purpose the durations computed from theoretical considerations for free-air conditions, such as those by Brode, are of little value since the complex effects of surface reflections are not considered. Thus, the semiempirical relations presented in Chap. 3 of *The Effects of Nuclear Weapons*[4] were used to define overpressure duration as a function of yield, overpressure, ambient pressure, and the speed of sound. Using data for both the surface burst and the "typical air burst," the following mathematical expression was derived

$$\log t_p^+ = 5.7995 + (1/3) \log W - 0.2957 \log p_s - 0.0376 \log p_0 - \log c_0 \tag{2.24}$$

where t_p^+ = duration of positive overpressure in milliseconds
W = yield in kilotons
p_s = shock overpressure in pounds per square inch
p_0 = ambient pressure in pounds per square inch
c_0 = velocity of sound in the undisturbed air in feet per second

The above equation reflects data for the surface burst for shock overpressure (sea-level conditions) from 1.68 to 36.7 psi and for the "typical air burst" from 1.86 to 19.7 psi.

(b) *Overpressure vs. Wind Duration.* Instrumentation used in past weapons tests was not refined enough to establish a relation between overpressure and wind duration. However, the theoretical work quoted above has established such a relation. Figure 2.2, derived from Brode's work,[1,3] presents the ratio of the wind duration to the pressure duration for overpresspures up to 3 atm (44.1 psi at sea level). It is apparent from this chart that for the higher overpressures air-particle inertia has the effect of sustaining positive winds for an appreciable time after the overpressure has become negative.

2.3.5 Velocity of Propagation of the Pressure Disturbance

It has been shown that it is necessary to know the velocity of propagation of the pressure disturbance in order to compute the motion of objects displaced by blast waves. An easily evaluated relation[5] that was used for this purpose is:

$$\dot{X} = \frac{3}{5} U + \sqrt{1 + \left(\frac{3}{5} U\right)^2} \tag{2.25}$$

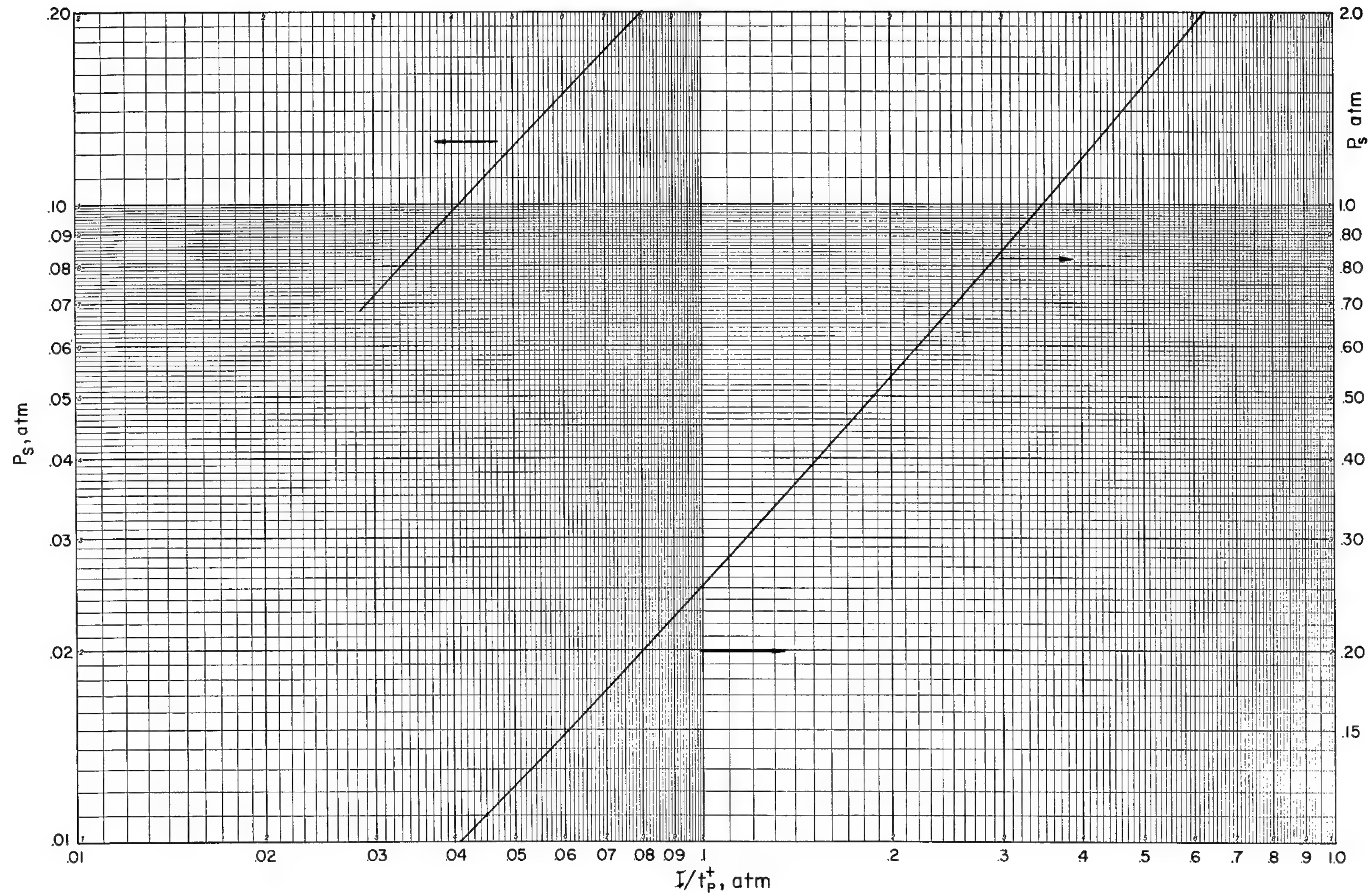

Fig. 2.1—Shock overpressure as a function of the ratio of overpressure impulse to overpressure duration.

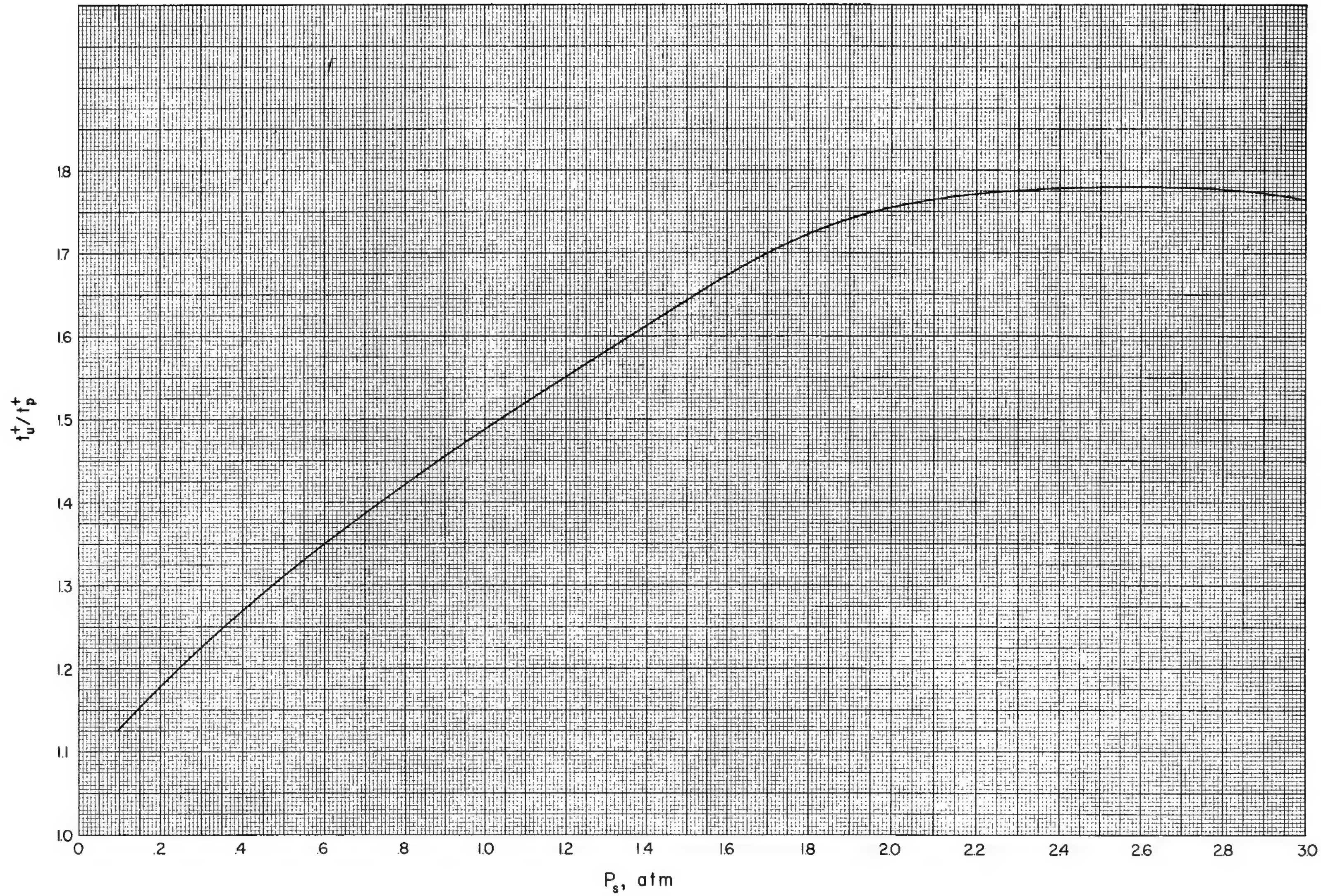

Fig. 2.2—Ratio of duration of wind to that of overpressure as a function of shock overpressure.

Two objections might be raised to the use of the above equation for the purposes of this study. First, it applies strictly to the speed of propagation of the shock front, not to pressure regions behind the front. Second, it was derived for nondivergent flow; whereas the present study applies to divergent flow. In spite of these limitations, the relation was found to be in reasonable agreement with work done by Brode[1,2] as quoted in Sec. 2.3.2.

This, added to the fact that X appears only in the time-correction term (see Eq. 2.7), whose effect on the computed value of dV is second order, probably justifies its use in the present context.

REFERENCES

1. Harold L. Brode, Numerical Solutions of Spherical Blast Waves, *J. Appl. Phys., 26:* 766-775 (June 1955).
2. Harold L. Brode, Point Source Explosion in Air, Report AECU-3517, The Rand Corporation, Dec. 3, 1956.
3. Harold L. Brode, personal communication.
4. Samuel Glasstone (Ed.), *The Effects of Nuclear Weapons*, Superintendent of Documents, U. S. Government Printing Office, Washington, D. C., June 1957.
5. Ascher H. Shapiro, *The Dynamics and Thermodynamics of Compressible Fluid Flow*, Vol. 2, p. 1001, Ronald Press Company, New York, 1954.

Chapter 3

COMPUTATIONAL METHOD

3.1 SCOPE OF COMPUTATIONAL EFFORT

Because computations were made in terms of dimensionless quantities, it was necessary to use only two independent variables: (1) the acceleration-coefficient numeric* ($A = \alpha p_0 t_u^+/c_0$) containing acceleration coefficient, ambient pressure, speed of sound, and duration of positive winds (yield dependent) and (2) the shock-overpressure numeric ($P_s = p_s/p_0$), which also involves the ambient pressure. Thus, five independent variables, one describing the object displaced and four describing the blast wave, were effectively reduced to two. It should be pointed out that the shock-overpressure numeric (along with the duration variable) represents or defines three other blast variables that are actually used in the computations; namely, dynamic-pressure numeric (Q), wind numeric (U), and propagation-velocity numeric ($\dot{X}$), all of which are functions of the time numeric ($Z = t/t_u^+$).

Thus, for computational purposes, it was necessary to set limits only on A and P_s. Consistent with the scope of the problem stated in Sec. 1.2, the limits arbitrarily set for A were 0.1 to 9000 and for P_s from 0.068 to 1.7 (1 psi to 25 psi for sea-level ambient pressure). Computations were made for 15 values of P_s within the stated range, and associated with each of these were 11 values of A (see Table 3.1, columns I and II), making a total of 165 complete numerical integrations.

3.2 GENERAL PLANNING

Figure 3.1 illustrates some of the considerations in planning for numerical solutions of the mathematical model. This plot shows the pertinent blast variables in dimensionless form as functions of the time numeric ($T = t/t_p^+$) for a 0.5-atm blast wave. Also shown on this plot are velocity ($V = v/c_0$) and displacement ($D = d/t_u^+c_0$) computed for an object with an acceleration coefficient ($A = \alpha p_0 t_u^+/c_0$) of 30. It should be noted that all plotted quantities change most rapidly at early times. This means that a stepwise solution should be started using small time increments, these to be lengthened as the solution progresses. Also of interest on this chart is the U′ curve, which represents the wind numeric at the position of the moving object rather than at a fixed position. At T = 0.5, missile velocity was equal to that of the wind, and so the integration was stopped. Sixty-two steps were taken to arrive at the solution shown here.

3.3 STEP SIZE

As shock overpressures increase, the rate of decay of the blast variables from shock values also increases. For mean-value assumptions (i.e., the assumption that the variable is constant with a value equal to the mean over a specified time increment) to be equally valid for

*Numeric is used here to designate a dimensionless quantity.

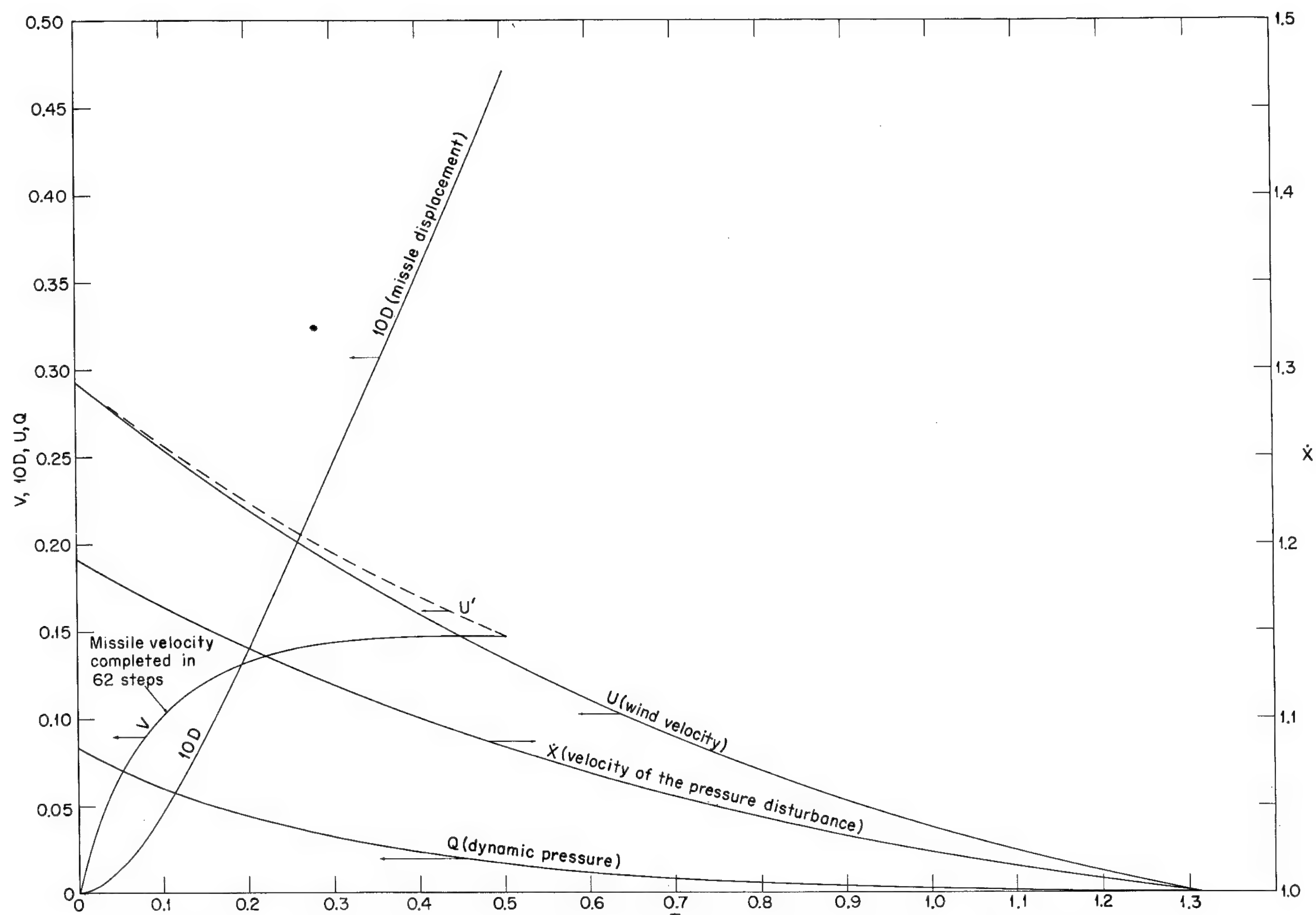

Fig. 3.1 — Blast and missile-motion parameters vs. time after arrival of blast wave computed for p_s = 0.5 atm, A = 30 (all quantities dimensionless). Q, U, and $\dot{X}$ curves represent blast parameters as they would be measured at the point of origin of the missile. The U′ curve represents the wind existing at the location of the moving missile indicated by the displacement (D) curve.

TABLE 3.1—INCREMENTAL VALUES OF THE INDEPENDENT VARIABLE AND PARAMETRIC VALUES FOR WHICH COMPUTATIONS WERE PERFORMED

I		II	III	IV
P_s	t_p^+/t_u^+	A	ΔT*	T_j†
0.068	0.900	0.1	0.0001	0.002
0.10	0.885	0.3	0.0002	0.004
0.15	0.875	1	0.0003	0.008
0.20	0.855	3	0.0004	0.015
0.25	0.840	10	0.001	0.030
0.30	0.835	30	0.002	0.060
0.35	0.805	100	0.003	0.120
0.40	0.793	300	0.005	0.250
0.50	0.760	1000	0.007	0.500
0.60	0.740	3000	0.010	0.750
0.70	0.720	9000	0.025	1.000
0.80	0.710		0.050	Final
1.00	0.675		0.100	
1.30	0.635			
1.70	0.585			

*Ten steps of each ΔT were used starting with $\Delta T = 0.001$. See Sec. 3.3 for an explanation of first four values of ΔT.

†T_j = times for which computed results were printed out.

high overpressures, the time increments should be correspondingly decreased. Noting that the ratio of overpressure duration to wind duration decreases for increasing overpressures (see Table 3.1, column I) suggested the use of a set of time increments in T constant for all solutions. The ΔZ values computed for each overpressure (using $\Delta Z = t_p^+/t_u^+ \, \Delta T$) then decrease as desired for the higher overpressure blast waves.

The first computation in each integration series was made for a time increment, ΔT, equal to 0.001. If the velocity V so computed was greater than 0.1, the solution was discarded; then ΔT values of 0.0001, 0.0002, 0.0003, and 0.0004 were used, in turn, and T = 0.001 was arrived at in four steps. Succeeding steps, gradually increasing in size, were then taken until the end of the integration (see Table 3.1). If the initial step, $\Delta T = 0.001$, yielded a velocity less than 0.1, the integration proceeded from there without the use of the shorter steps.

The shortest integration, using the system described above, required 14 steps; this was for $P_s = 1.7$, A = 9000. In general, the number of steps required increased as A decreased; e.g., 75 steps were required for A = 3.0 and $P_s = 0.068$ and 81 steps were required for A = 0.1 and $P_s = 1.7$.

3.4 MACHINE OUTPUT*

Since printing out results at the end of each step would have slowed the computation considerably and also would have produced much more information than could have been utilized, it was decided to limit the output of intermediate results to those necessary for the preparation of accurate plots. Because of the time-correction term (see Sec. 2.2.2), time at the end of any particular step was different for each set of conditions. For simplicity in monitoring results and ease of plotting time histories, it was convenient to program output at a set of preselected time (see Table 3.1, column IV). Thus, it was necessary to program the computer to interpolate (linearly) the computed results between time steps to the times selected for print-out.

Special problems arose in the determination of the final values of the computed results; i.e., the values occurring at the time when missile velocity and wind velocity were identical.

*The computer, a CRC-102A, was generously made available by Sandia Corporation.

Since missile velocity changes very slowly near the end of the accelerative phase, it was sufficiently accurate to take final or maximum missile velocity to be that computed for the first step where it equaled or exceeded the wind velocity. However, it was necessary to obtain the time at which this occurred by interpolating the wind values to a time when they equaled maximum missile velocity. Making use of this time, displacement at maximum velocity could then be computed. Final acceleration was always, of course, zero.

3.5 DISCUSSION OF ERROR

The usable word length of the computer was 36 binary digits or the equivalent of 9 decimal digits of input or output. The fixed-point fractional mode of operation required careful scaling of all magnitudes (primarily because of the large range of the parameter A) so that sufficient significance be retained without the need for rescaling. Binary scaling proved adequately conservative in the attainment of this objective.

Approximations for square roots and cube roots were obtained with accuracy greater than eight decimal places, and the exponential approximation is reported to be accurate to ±2 in the seventh decimal place. (Cube roots were obtained by the Newton-Raphson method,[1] and the exponential, by the rational polynomial approximation.[2])

Blast-wave parameters were evaluated from empirical equations that were derived by fitting curves to computed data obtained from a blast-wave model.[3,4] Although Brode did not make a definite statement regarding the over-all accuracy of the blast model, he did indicate some deviation of the empirical equations from the computed data. From this it can be surmised that computations involved in the present problem were carried out as accurately as was warranted by the accuracy of the input blast data as well as by the probity of the missile model itself (see Sec. 1.2).

It is noteworthy that computed missile velocity becomes stable by virtue of the number of steps involved in each integration; i.e., if for some reason computed missile velocity at the end of a particular step is too low, the net wind velocity $(U - V)$ used in the next step will be correspondingly high, thereby tending to compensate for the original error. As a consequence the final solution is not extremely sensitive to the magnitude of the time increments so long as, within any particular solution, the steps are sufficiently numerous for the compensatory effect to be realized before the computation ends.

REFERENCES

1. J. B. Scarborough, *Numerical Mathematical Analysis*, pp. 192-194, Johns Hopkins Press, Baltimore, Md., 1955.
2. C. Hastings, Jr., *Approximations for Digital Computers*, Princeton University Press, Princeton, N. J., 1955.
3. Harold L. Brode, Numerical Solutions of Spherical Blast Waves, *J. Appl. Phys., 26:* 766-775 (June 1955).
4. Harold L. Brode, Point-source Explosion in Air, Report AECU-3517, The Rand Corporation, Dec. 3, 1956.

Chapter 4

RESULTS: COMPUTED MOTION PARAMETERS FOR OBJECTS DISPLACED BY CLASSICAL BLAST WAVES

The results of the 153 numerical integrations are presented in Table 4.1 in terms of the dimensionless parameters. Each integration was made for a specific combination of overpressure (P) and acceleration coefficient (A). Values of missile velocity (V), distance of travel (D), and missile acceleration (V) are given for 13 times during the accelerative phase of missile displacement. Numbers appearing in parenthesis after V, D, and V are scaling factors indicating the number of places the decimal point has been moved to the right. Consider, for example, the data tabulated for P = 0.10 and A = 1000 at T = 0.120. In this instance V(6) is read as 55677, and thus V = 0.055677.

At T = 0, the time of arrival of the blast wave, velocity and displacement are zero, but acceleration is maximum. "T = Final" is defined as the time after arrival of the blast wave when missile velocity is maximum and acceleration is zero. The displacement (D) tabulated under "Final" is defined as the total displacement of the object at the instant when the velocity is maximum. The actual time when maximum velocity is attained appears in the last column under "T_{final}."

It should be noted that the time measurements used in this table are normalized with respect to the duration of the positive pressure phase. Since the duration of positive winds is longer than that of the positive pressure, T_{final} values are sometimes greater than unity. The exact value of T_{final} is, of course, the time when the missile velocity equals the wind velocity.

Examples of uses of the tabulated data along with various plots are given in Chap. 5.

TABLE 4.1—COMPUTED MOTION PARAMETERS FOR OBJECTS DISPLACED BY CLASSICAL BLAST WAVES

Nomenclature (Parameters can be evaluated in any consistent system of units):

- $\alpha = sC_D / m$
- $A = \alpha p_o t_u^+ / c_o$
- c_o = velocity of sound in undisturbed air
- C_D = drag coefficient of moving object
- d = displacement of object
- $D(n) = d / (t_u^+ c_o) \times 10^n$
- m = mass of moving object
- p_m = maximum overpressure
- p_o = pressure of undisturbed air
- $P = p_m / p_o$
- s = area presented to wind by object
- t_p^+ = positive overpressure duration
- t_u^+ = positive wind duration
- $T = t / t_p^+$
- v = velocity of moving object
- $V(n) = v / c_o \times 10^n$
- $\dot{v}$ = acceleration of moving object
- $\dot{V}(n) = \dot{v} t_u^+ / c_o \times 10^n$

P	A	T:	0	.002	.004	.008	.015	.030	.060	.120	.250	.500	.750	1.000	Final	T_{final}
		V (7):	0	88	175	345	635	1218	2253	3912	6333	8820	9941	10296	10312	
.068	3	D (8):	0	1	3	12	44	169	641	2327	8439	25850	47142	70020	78517	1.092
		$\dot{V}$ (7):	49066	48500	47950	46860	45040	41460	35410	26640	16090	7350	2990	450	0	
		V (7):	0	293	582	1149	2109	4038	7433	12801	20435	27852	30821		31449	
	10	D (7):	0		1	4	14	56	212	766	2750	8303	14963		22561	1.020
		$\dot{V}$ (6):	16355	16155	15958	15573	14930	13670	11560	8541	4970	2080	693		0	
		V (7):	0	877	1741	3433	6278	11930	21674	36500	56161	72687	77374		77687	
	30	D (7):	0	1	3	12	43	167	625	2219	7761	22595	39619		49734	0.895
		$\dot{V}$ (6):	49066	48359	47666	46319	44085	39766	32709	22998	12132	3979	645		0	
		V (6):	0	291	576	1127	2037	3777	6578	10369	14477	16736			16896	
	100	D (7):	0	3	10	41	141	537	1952	6613	21514	57390			84057	0.676
		$\dot{V}$ (5):	16355	15998	15651	14987	13915	11942	8989	5442	2159	293			0	
		V (6):	0	864	1692	3245	5674	9907	15714	21879	26410				27340	
	300	D (7):	0	8	31	120	403	1468	4990	15361	44252				94925	0.458
		$\dot{V}$ (5):	49066	46971	45000	41392	35994	27296	16832	7547	1650				0	
		V (6):	0	2776	5253	9478	15143	22942	30579	35809	37497				37500	
	1000	D (7):	0	25	98	366	1151	3772	11148	29385	72750				79332	0.270
		$\dot{V}$ (4):	16355	14546	13015	10583	7675	4336	1807	466	5				0	
		V (6):	0	7549	13179	20999	28954	36776	41926	43909					43993	
	3000	D (7):	0	71	259	884	2484	7005	17782	41155					56458	0.159
		$\dot{V}$ (4):	49066	35858	27310	17282	9279	3569	948	75					0	
		V (6):	0	17670	26508	35305	41625	46042	47903						48084	
	9000	D (7):	0	175	579	1712	4167	10150	22914						36728	0.092
		$\dot{V}$ (3):	14720	6565	3687	1618	621	164	20						0	
		V (7):	0	186	370	732	1346	2586	4797	8373	13662	19090	21447	22143	22172	
.10	3	D (7):	0		1	3	9	35	134	488	1780	5484	10009	14854	16451	1.081
		$\dot{V}$ (6):	10563	10446	10331	10105	9727	8981	7720	5874	3592	1607	617	79	0	
		V (7):	0	619	1231	2433	4466	8550	15748	27142	43334	58605	64117		65030	
	10	D (7):	0	1	2	9	30	117	442	1596	5735	17274	30974		44789	0.991
		$\dot{V}$ (6):	35211	34780	34357	33530	32151	29451	24934	18455	10662	4157	1159		0	
		V (6):	0	186	368	725	1324	2507	4527	7550	11421	14366	14980		14990	
	30	D (7):	0	2	7	26	90	345	1288	4545	15714	44931	77637		87959	0.828
		$\dot{V}$ (5):	10563	10400	10240	9930	9418	8437	6853	4713	2352	630	40		0	
		V (6):	0	615	1214	2364	4238	7745	13170	20056	26737	29507			29549	
	100	D (6):	0	1	2	9	29	109	391	1291	4051	10392			12684	0.588
		$\dot{V}$ (5):	35211	34274	33371	31661	28948	24111	17254	9631	3229	166			0	
		V (6):	0	1815	3527	6674	11421	19217	28969	38092	43502				44039	
	300	D (6):	0	2	6	25	81	287	940	2759	7546				12672	0.382
		$\dot{V}$ (4):	10563	9957	9398	8408	7002	4921	2717	1042	148				0	
		V (6):	0	5730	10604	18439	28080	39911	49951	55677					56779	
	1000	D (7):	0	52	197	717	2179	6786	18945	47387					97492	0.220
		$\dot{V}$ (4):	35211	29769	25479	19234	12654	6243	2219	430					0	
		V (6):	0	14926	24836	37145	48177	57673	63035	64483					64485	
	3000	D (7):	0	140	496	1613	4298	11440	27641	61685					66790	0.129
		$\dot{V}$ (3):	10563	6740	4663	2596	1225	408	88	1					0	
		V (6):	0	32061	44935	56140	63298	67740	69201						69239	
	9000	D (7):	0	323	1015	2836	6574	15342	33599						42608	0.075
		$\dot{V}$ (3):	31690	10438	5105	1957	672	153	9						0	
		V (7):	0	137	273	540	994	1916	3574	6298	10428	14752	16649	17259	17290	
.15	1	D (7):	0			2	7	26	98	360	1330	4146	7613	11338	13067	1.114
		$\dot{V}$ (7):	78671	77860	77070	75510	72890	67720	58890	45730	28730	13000	5130	970	0	
		V (7):	0	411	817	1617	2976	5727	10648	18654	30564	42539	47360	48571	48610	
	3	D (7):	0		1	6	20	77	294	1072	3927	12109	22033	32571	35280	1.064
		$\dot{V}$ (6):	23601	23347	23097	22607	21787	20168	17418	13352	8165	3461	1188	93	0	
		V (6):	0	137	272	537	985	1885	3466	5954	9430	12492	13406		13491	
	10	D (7):	0	1	5	19	66	255	963	3469	12410	36978	65553		87180	0.934
		$\dot{V}$ (6):	78671	77685	76716	74829	71681	65535	55283	40583	22700	7722	1498		0	
		V (6):	0	409	812	1595	2903	5459	9741	15930	23339	28069			28614	
	30	D (6):	0		1	6	19	75	276	962	3251	9009			14907	0.737
		$\dot{V}$ (5):	23601	23188	22784	22005	20728	18311	14505	9531	4283	787			0	
		V (6):	0	1353	2659	5140	9097	16235	26597	38527	48331				50886	
	100	D (6):	0	1	5	18	62	230	802	2548	7610				18291	0.493
		$\dot{V}$ (5):	78671	75942	73342	68503	61051	48440	32022	15799	4053				0	
		V (6):	0	3959	7601	14071	23308	37233	52609	64838	70129				70248	
	300	D (6):	0	4	14	52	167	572	1776	4920	12715				16408	0.310
		$\dot{V}$ (4):	23601	21681	19979	17107	13344	8421	4021	1251	71				0	
		V (6):	0	12152	21747	35909	51461	68068	80049	85424					85866	
	1000	D (6):	0	11	41	143	415	1215	3191	7580					11803	0.176
		$\dot{V}$ (4):	78671	61322	49088	33388	19384	8167	2417	287					0	

TABLE 4.1—COMPUTED MOTION PARAMETERS FOR OBJECTS DISPLACED BY CLASSICAL BLAST WAVES (Continued)

P	A	T:	0	.002	.004	.008	.015	.030	.060	.120	.250	.500	.750	1.000	Final	T_{final}
		V (6):	0	29712	46419	64522	78639	89205	94174						94913	
.15	3000	D (7):	0	281	957	2937	7384	18539	42794						78423	0.103
		$\dot{V}$ (3):	23601	12265	7478	3581	1471	422	67						0	
		V (5):	0	5724	7468	8791	9543	9952							10040	
	9000	D (7):	0	594	1768	4656	10315	23180							49210	0.060
		$\dot{V}$ (3):	70804	15437	6494	2178	671	124							0	
		V (8):	0	709	1412	2797	5159	9972	18694	33219	55666	79530	90144	93841	94326	
.20	.3	D (8):	0	1	2	10	34	131	501	1847	6879	21660	39963	59715	75430	1.195
		$\dot{V}$ (7):	41667	41270	40880	40120	38830	36280	31870	25160	16130	7380	3000	750	0	
		V (7):	0	236	470	932	1718	3318	6211	11005	18345	25994	29258	30281	30336	
	1	D (7):	0		1	3	11	44	167	613	2275	7125	13085	19477	22777	1.127
		$\dot{V}$ (6):	13889	13754	13620	13360	12921	12050	10551	8277	5237	2321	886	169	0	
		V (7):	0	709	1410	2791	5140	9905	18458	32445	53308	73877	81694	83460	83509	
	3	D (7):	0	1	2	10	33	130	497	1818	6679	20600	37382	55103	59218	1.058
		$\dot{V}$ (6):	41667	41233	40806	39970	38568	35793	31048	23932	14589	5913	1872	108	0	
		V (6):	0	236	469	926	1699	3246	5958	10200	16013	20819	22032		22099	
	10	D (6):	0		1	3	11	43	162	582	2072	6108	10725		13452	0.894
		$\dot{V}$ (5):	13889	13711	13537	13198	12632	11527	9687	7043	3807	1145	156		0	
		V (6):	0	706	1397	2741	4971	9290	16389	26321	37483	43582			43974	
	30	D (6):	0	1	2	9	33	125	458	1573	5210	14074			20710	0.677
		$\dot{V}$ (5):	41667	40854	40063	38542	36066	31440	24313	15301	6234	784			0	
		V (6):	0	2324	4550	8730	15269	26672	42325	58939	70827				72901	
	100	D (6):	0	2	8	31	103	375	1277	3931	11310				22876	0.437
		$\dot{V}$ (4):	13889	13299	12743	11726	10203	7746	4781	2129	430				0	
		V (6):	0	6744	12803	23233	37417	57327	77289	91341	95988				95997	
	300	D (6):	0	6	23	85	268	888	2651	7054	17590				19256	0.270
		$\dot{V}$ (4):	41667	37336	33631	27665	20384	11787	5046	1336	14				0	
		V (5):	0	2017	3504	5549	7607	9598	10884	11356					11371	
	1000	D (6):	0	18	66	223	623	1747	4410	10160					13346	0.153
		$\dot{V}$ (3):	13889	10028	7569	4729	2501	946	245	16					0	
		V (5):	0	4669	6954	9200	10795	11887	12336						12373	
	3000	D (7):	0	441	1452	4268	10327	25025	56278						87144	0.089
		$\dot{V}$ (3):	41667	18053	9993	4311	1624	423	49						0	
		V (5):	0	8302	10362	11795	12545	12921							12976	
	9000	D (7):	0	867	2491	6329	13659	30061							54150	0.052
		$\dot{V}$ (2):	12500	1959	745	230	67	10							0	
		V (7):	0	108	215	427	788	1526	2869	5122	8633	12351	13974	14533	14611	
.25	.3	D (7):	0			1	5	20	75	279	1044	3299	6089	9095	11534	1.199
		$\dot{V}$ (7):	64655	64070	63500	62370	60480	56690	50100	39890	25720	11590	4620	1170	0	
		V (7):	0	360	717	1422	2623	5074	9522	16940	28356	40143	45027	46504	46632	
	1	D (7):	0		1	5	17	65	250	925	3445	10810	19837	29489	34777	1.135
		$\dot{V}$ (6):	21552	21351	21154	20767	20114	18813	16556	13078	8287	3585	1321	244	0	
		V (6):	0	108	215	426	784	1513	2823	4971	8168	11245	12346	12566	12571	
	3	D (7):	0	1	4	14	50	195	745	2733	10052	30943	55942	82193	86992	1.045
		$\dot{V}$ (6):	64655	63999	63352	62086	59957	55734	48467	37432	22617	8734	2533	91	0	
		V (6):	0	360	715	1411	2586	4935	9034	15389	23897	30479	31872		31910	
	10	D (6):	0		1	5	17	64	242	866	3061	8918	15513		18373	0.857
		$\dot{V}$ (5):	21552	21268	20990	20448	19546	17787	14861	10662	5542	1469	126		0	
		V (6):	0	1074	2126	4161	7520	13956	24332	38369	53178	60127			60345	
	30	D (6):	0	1	4	14	49	185	674	2284	7414	19566			26056	0.628
		$\dot{V}$ (5):	64655	63256	61899	59300	55100	47358	35710	21496	7949	638			0	
		V (6):	0	3528	6880	13102	22646	38751	59733	80440	93498				95022	
	100	D (6):	0	3	12	45	151	544	1809	5419	15118				26728	0.396
		$\dot{V}$ (4):	21552	20464	19452	17631	14981	10901	6316	2564	406				0	
		V (5):	0	1015	1906	3393	5326	7874	10230	11727					12110	
	300	D (6):	0	9	33	123	383	1231	3559	9182					21572	0.243
		$\dot{V}$ (4):	64655	56495	49759	39389	27546	14769	5777	1323					0	
		V (5):	0	2959	5005	7645	10121	12330	13642	14043					14045	
	1000	D (6):	0	26	94	310	841	2279	5591	12612					14590	0.137
		$\dot{V}$ (3):	21552	14433	10322	5995	2938	1026	238	6					0	
		V (5):	0	6521	9346	11921	13615	14711	15106						15123	
	3000	D (7):	0	617	1974	5614	13207	31215	68967						94176	0.080
		$\dot{V}$ (3):	64655	23671	12102	4817	1713	409	32						0	
		V (5):	0	10886	13173	14661	15394	15735							15768	
	9000	D (7):	0	1144	3200	7928	16810	36491							58110	0.046
		$\dot{V}$ (2):	19397	2292	807	234	65	8							0	
		V (7):	0	152	302	600	1108	2150	4054	7268	12307	17623	19908	20690	20804	
.30	.3	D (7):	0			2	7	27	104	388	1457	4617	8524	12729	16174	1.201
		$\dot{V}$ (6):	9247	9168	9090	8937	8678	8160	7249	5814	3762	1673	657	170	0	
		V (7):	0	506	1008	1998	3690	7146	13443	23996	40294	56964	63694	65668	65841	
	1	D (7):	0		2	7	23	90	347	1283	4797	15073	27633	41028	48756	1.142
		$\dot{V}$ (6):	30822	30548	30277	29746	28849	27054	23912	18990	12031	5091	1819	328	0	
		V (6):	0	152	302	598	1103	2128	3975	7008	11505	15732	17162		17414	
	3	D (6):	0			2	7	27	103	378	1391	4272	7695		11771	1.035
		$\dot{V}$ (6):	92446	91547	90641	88868	85880	79935	69639	53809	32177	11873	3175		0	
		V (6):	0	505	1003	1980	3627	6911	12616	21374	32820	41136	42616		42633	
	10	D (6):	0		2	7	23	88	332	1186	4162	11986	20680		23309	0.825
		$\dot{V}$ (5):	30822	30404	29994	29196	27868	25283	20989	14847	7420	1741	84		0	

TABLE 4.1—COMPUTED MOTION PARAMETERS FOR OBJECTS DISPLACED BY CLASSICAL BLAST WAVES (Continued)

P	A	T:	0	.002	.004	.008	.015	.030	.060	.120	.250	.500	.750	1.000	Final	T_{final}
		V (6):	0	1507	2979	5820	10481	19319	33295	51603	69808	77210			77317	
.30	30	D (6):	0	1	5	20	67	253	913	3055	9739	25202			30955	0.590
		V̇ (5):	92466	90267	88139	84084	77580	65751	48368	27908	9431	450			0	
		V (5):	0	493	959	1812	3097	5199	7811	10227	11592				11700	
	100	D (6):	0	4	16	62	205	726	2369	6931	18862				30043	0.366
		V̇ (4):	30822	29024	27372	24446	20304	14203	7778	2916	362				0	
		V (5):	0	1408	2615	4574	7018	10069	12707	14243					14554	
	300	D (6):	0	12	45	165	505	1584	4456	11223					23530	0.223
		V̇ (4):	92466	78821	67944	51892	34628	17406	6319	1269					0	
		V (5):	0	4007	6614	9801	12613	14977	16288	16622					16623	
	1000	D (6):	0	35	124	400	1057	2791	6701	14888					15638	0.125
		V̇ (3):	30822	19210	13089	7141	3298	1080	227	1					0	
		V (5):	0	8452	11745	14572	16324	17411	17755						17762	
	3000	D (6):	0	80	250	692	1593	3697	8066						10009	0.073
		V̇ (3):	92466	29055	13911	5196	1770	393	19						0	
		V (5):	0	13411	15882	17400	18113	18421							18440	
	9000	D (7):	0	1523	3982	9527	19826	42498							61565	0.043
		V̇ (2):	27740	2584	852	236	63	6							0	
		V (7):	0	200	399	792	1465	2845	5380	9689	16489	23665	26730	27787	27954	
.35	.3	D (7):	0		1	3	9	35	135	503	1898	6037	11155	16664	21476	1.214
		V̇ (6):	12500	12399	12300	12104	11773	11105	9919	8014	5213	2304	902	244	0	
		V (7):	0	668	1330	2638	4874	9455	17828	31936	53819	76087	84941	87520	87766	
	1	D (7):	0	1	2	9	30	117	448	1662	6236	19633	35989	53412	64400	1.156
		V̇ (6):	41667	41314	40965	40280	39119	36786	32661	26086	16555	6909	2433	451	0	
		V (6):	0	200	399	790	1456	2812	5259	9284	15239	20735	22522		22817	
	3	D (6):	0		1	3	9	35	133	488	1798	5512	9904		15059	1.032
		V̇ (5):	12500	12379	12260	12026	11631	10842	9465	7321	4343	1549	392		0	
		V (6):	0	666	1323	2610	4778	9094	16560	27922	42468	52503	54045		54051	
	10	D (6):	0	1	2	8	29	114	426	1517	5291	15092	25877		28159	0.802
		V̇ (5):	41667	41088	40520	39416	37577	34002	28070	19607	9475	2010	54		0	
		V (6):	0	1986	3922	7647	13727	25146	42895	65500	86877	94593			94626	
	30	D (6):	0	2	6	25	86	322	1156	3827	12011	30607			35439	0.563
		V̇ (4):	12500	12178	11867	11278	10338	8651	6225	3462	1084	29			0	
		V (5):	0	648	1255	2356	3986	6582	9678	12393	13795				13873	
	100	D (6):	0	5	21	79	259	908	2912	8356	22309				32959	0.345
		V̇ (4):	41667	38931	36446	32114	26131	17658	9221	3240	321				0	
		V (5):	0	1836	3376	5812	8748	12247	15113	16674					16934	
	300	D (6):	0	15	57	207	623	1917	5281	13059					25233	0.210
		V̇ (3):	12500	10412	8801	6512	4174	1991	683	123					0	
		V (5):	0	5110	8261	11945	15031	17522	18828						19114	
	1000	D (6):	0	44	153	485	1257	3251	7681						16550	0.118
		V̇ (3):	41667	24324	15896	8237	3639	1133	220						0	
		V (5):	0	10385	14091	17125	18918	19993	20302						20305	
	3000	D (6):	0	97	298	809	1834	4200	9082						10523	0.069
		V̇ (2):	12500	3439	1561	555	183	39	1						0	
		V (5):	0	15854	18478	20011	20716	20998							21011	
	9000	D (7):	0	1799	4610	10861	22381	47630							64499	0.040
		V̇ (2):	37500	2863	897	242	61	5							0	
		V (7):	0	85	170	338	625	1216	2308	4176	7152	10315	11679	12169	12276	
.40	.1	D (8):	0	1	3	11	38	147	569	2126	8072	25810	47818	71554	99719	1.290
		V̇ (6):	5405	5365	5324	5245	5110	4837	4346	3542	2326	1035	413	124	0	
		V (7):	0	256	510	1013	1874	3646	6909	12481	21305	30570	34470	35803	36019	
	.3	D (7):	0		1	3	11	44	170	636	2410	7679	14187	21181	27648	1.227
		V̇ (6):	16216	16092	15969	15727	15315	14481	12986	10544	6866	2996	1157	314	0	
		V (6):	0	85	170	337	624	1211	2287	4107	6931	9775	10879	11191	11220	
	1	D (7):	0	1	3	11	37	147	565	2102	7902	24880	45545	67506	81618	1.159
		V̇ (6):	54054	53613	53177	52320	50864	47924	42680	34193	21638	8843	3026	542	0	
		V (6):	0	256	509	1009	1861	3596	6730	11882	19456	26282	28390		28705	
	3	D (6):	0		1	3	11	44	167	615	2265	6918	12385		18505	1.020
		V̇ (5):	16216	16062	15909	15609	15102	14087	12304	9501	5565	1900	445		0	
		V (6):	0	851	1690	3332	6095	11580	21018	35224	52969	64529	66013		66017	
	10	D (6):	0	1	3	11	37	143	534	1893	6554	18495	31501		32888	0.776
		V̇ (5):	54054	53278	52516	51035	48573	43790	35884	24677	11475	2164	17		0	
		V (5):	0	254	500	973	1740	3167	5343	8033	10449	11215			11216	
	30	D (6):	0	2	8	31	107	402	1429	4678	14454	36285			39581	0.537
		V̇ (4):	16216	15763	15327	14503	13201	10894	7656	4095	1183	13			0	
		V (5):	0	825	1591	2966	4966	8064	11617	14573	15964				16015	
	100	D (6):	0	7	26	99	321	1109	3499	9858	25862				35565	0.326
		V̇ (4):	54054	50090	46531	40426	32208	21021	10478	3453	261				0	
		V (5):	0	2318	4220	7151	10567	14457	17496	19044					19255	
	300	D (6):	0	19	71	254	753	2271	6139	14938					26743	0.198
		V̇ (3):	16216	13187	10925	7832	4828	2196	713	114					0	
		V (5):	0	6310	9999	14135	17440	20014	21289						21529	
	1000	D (6):	0	54	185	576	1465	3724	8678						17359	0.111
		V̇ (3):	54054	29529	18538	9154	3887	1155	207						0	
		V (5):	0	12379	16446	19635	21444	22492	22762						22763	
	3000	D (6):	0	116	349	930	2080	4709	10108						10979	0.065
		V̇ (2):	16216	3921	1695	576	185	37							0	

TABLE 4.1—COMPUTED MOTION PARAMETERS FOR OBJECTS DISPLACED BY CLASSICAL BLAST WAVES (Continued)

P	A	T:	0	.002	.004	.008	.015	.030	.060	.120	.250	.500	.750	1.000	Final	T_{final}
		V (5):	0	18272	21013	22542	23232	23486							23493	
.40	9000	D (7):	0	2086	5253	12216	24965	52810							67114	0.038
		V̇ (2):	48649	3081	919	243	59	3							0	
		V (7):	0	126	252	500	926	1808	3445	6279	10842	15700	17784	18546	18737	
.50	.1	D (7):	0			2	5	21	81	305	1166	3750	6962	10427	14825	1.310
		V̇ (6):	8333	8277	8222	8112	7925	7541	6835	5637	3733	1652	660	209	0	
		V (7):	0	379	755	1499	2777	5416	10310	18748	32238	46383	52281	54316	54742	
	.3	D (7):	0		1	5	16	63	243	912	3477	11134	20596	30763	42156	1.274
		V̇ (6):	25000	24828	24657	24321	23745	22564	20403	16744	10974	4744	1823	521	0	
		V (6):	0	126	251	499	924	1797	3407	6149	10422	14680	16291	16739	16786	
	1	D (6):	0			2	5	21	81	301	1135	3582	6551	9701	11991	1.180
		V̇ (6):	83333	82710	82092	80874	78794	74546	66825	53929	34108	13611	4542	837	0	
		V (6):	0	378	753	1492	2754	5325	9979	17633	28792	38517	41321		41691	
	3	D (6):	0		1	5	16	62	238	875	3219	9784	17431		25665	1.010
		V̇ (5):	25000	24770	24543	24096	23338	21806	19081	14709	8459	2720	577		0	
		V (6):	0	1257	2495	4916	8978	17010	30702	50930	75199	89664			91114	
	10	D (6):	0	1	4	15	52	201	751	2643	9037	25084			41899	0.744
		V̇ (5):	83333	82071	80833	78427	74431	66692	53969	36155	15816	2500			0	
		V (5):	0	374	736	1426	2536	4560	7550	11068	13977				14736	
	30	D (6):	0	3	11	44	150	559	1962	6299	18986				46961	0.503
		V̇ (4):	25000	24203	23440	22011	19783	15935	10756	5400	1377				0	
		V (5):	0	1210	2316	4266	7015	11082	15453	18806	20176				20198	
	100	D (6):	0	9	36	137	440	1491	4579	12540	32074				40074	0.302
		V̇ (4):	83333	76067	69685	59047	45357	27936	12931	3867	175				0	
		V (5):	0	3350	5992	9889	14180	18740	22055	23584					23731	
	300	D (6):	0	26	98	343	993	2907	7632	18145					29349	0.182
		V̇ (3):	25000	19466	15572	10581	6127	2588	775	101					0	
		V (5):	0	8772	13461	18387	22041	24735	25977						26158	
	1000	D (6):	0	73	245	739	1829	4528	10350						18758	0.102
		V̇ (3):	83333	40540	23831	10903	4371	1220	191						0	
		V (5):	0	16256	20959	24368	26234	27243							27462	
	3000	D (6):	0	156	445	1144	2500	5564							11778	0.060
		V̇ (2):	25000	4890	1951	629	191	35							0	
		V (5):	0	22867	25819	27343	28009	28228							28230	
	9000	D (7):	0	2584	6340	14474	29240	61350							71606	0.035
		V̇ (2):	75000	3527	973	249	57	2							0	
		V (7):	0	175	348	693	1285	2512	4805	8800	15268	22113	25002	26050	26325	
.60	.1	D (7):	0		1	2	7	28	110	415	1594	5139	9539	14279	20689	1.330
		V̇ (6):	11842	11770	11699	11557	11314	10807	9858	8189	5434	2368	933	299	0	
		V (7):	0	524	1045	2077	3852	7525	14372	26250	45311	65121	73208	75953	76552	
	.3	D (7):	0		2	6	22	85	329	1239	4746	15223	28139	41990	58498	1.292
		V̇ (6):	35526	35304	35082	34643	33888	32322	29394	24275	15905	6741	2536	724	0	
		V (6):	0	175	348	691	1280	2495	4741	8580	14555	20398	22528	23091	23148	
	1	D (6):	0		1	2	7	28	109	408	1543	4861	8868	13102	16217	1.182
		V̇ (5):	11842	11759	11677	11514	11235	10659	9593	7763	4872	1879	600	104	0	
		V (6):	0	523	1042	2065	3812	7374	13817	24382	39565	52265	55616		55989	
	3	D (6):	0		2	6	21	84	321	1179	4325	13048	23105		32969	0.988
		V̇ (5):	35526	35205	34887	34260	33192	31022	27119	20772	11645	3485	649		0	
		V (5):	0	174	345	679	1238	2336	4187	6863	9934	11600			11724	
	10	D (6):	0	1	5	20	70	270	1002	3497	11793	32183			50288	0.709
		V̇ (4):	11842	11651	11463	11098	10495	9331	7435	4832	1979	255			0	
		V (5):	0	516	1014	1957	3456	6138	9973	14261	17542				18240	
	30	D (6):	0	4	15	59	200	739	2558	8057	23730				53438	0.472
		V̇ (4):	35526	34242	33021	30752	27269	21412	13869	6545	1468				0	
		V (5):	0	1661	3157	5741	9278	14280	19338	22955	24240				24247	
	100	D (6):	0	12	48	181	575	1907	5716	15274	38258				43920	0.282
		V̇ (3):	11842	10641	9609	7939	5883	3430	1487	406	9				0	
		V (5):	0	4532	7966	12826	17890	22992	26456	27914					28011	
	300	D (6):	0	35	128	441	1250	3562	9130	21309					31570	0.170
		V̇ (3):	35526	26463	20454	13213	7247	2864	801	84					0	
		V (5):	0	11430	17048	22631	26516	29252	30426						30558	
	1000	D (6):	0	94	308	907	2196	5324	11988						19952	0.095
		V̇ (2):	11842	5146	2850	1219	466	123	17						0	
		V (5):	0	20161	25382	28914	30780	31741							31917	
	3000	D (6):	0	194	538	1353	2909	6393							12456	0.056
		V̇ (2):	35526	5718	2124	656	192	32							0	
		V (5):	0	27313	30406	31899	32525	32714							32714	
	9000	D (7):	0	3083	7414	16684	33410	69669							75464	0.032
		V (1):	10658	384	99	25	5								0	
		V (7):	0	228	455	905	1678	3280	6264	11447	19774	28472	32092	33402	33790	
.70	.1	D (7):	0		1	3	9	36	140	526	2014	6467	11968	17885	27204	1.384
		V̇ (6):	15909	15810	15711	15516	15179	14481	13175	10889	7151	3065	1196	388	0	
		V (7):	0	685	1366	2714	5030	9821	18729	34116	58594	83649	93707	97100	97878	
	.3	D (7):	0		2	8	27	108	418	1570	5992	19123	35233	52470	74779	1.317
		V̇ (6):	47727	47418	47111	46502	45455	43288	39247	32221	20859	8669	3220	930	0	
		V (6):	0	228	455	903	1672	3254	6169	11118	18726	26006	28589	29257	29325	
	1	D (6):	0		1	3	9	36	138	515	1941	6073	11030	16253	20284	1.191
		V̇ (5):	15909	15793	15677	15449	15057	14252	12767	10242	6318	2366	736	127	0	

TABLE 4.1—COMPUTED MOTION PARAMETERS FOR OBJECTS DISPLACED BY CLASSICAL BLAST WAVES (Continued)

P	A	T:	0	.002	.004	.008	.015	.030	.060	.120	.250	.500	.750	1.000	Final	T_{final}
		V (6):	0	684	1361	2696	4970	9593	17900	31353	50269	65532	69320		69708	
.70	3	D (6):	0		2	8	27	106	405	1483	5392	16090	28317		39757	0.978
		$\dot{V}$ (5):	47727	47265	46807	45907	44377	41283	35773	26965	14672	4164	718		0	
		V (5):	0	227	500	884	1607	3016	5352	8641	12259	14091			14200	
	10	D (6):	0	2	7	26	89	340	1254	4332	14375	38619			57995	0.690
		$\dot{V}$ (4):	15909	15624	15344	14805	13917	12228	9544	5997	2323	259			0	
		V (5):	0	673	1319	2534	4441	7786	12411	17350	20895				21555	
	30	D (6):	0	5	19	75	252	920	3142	9713	28030				59489	0.454
		$\dot{V}$ (4):	47727	45771	43925	40531	35415	27071	16841	7529	1538				0	
		V (5):	0	2154	4065	7302	11612	17452	23080	26882	28088				28091	
	100	D (6):	0	16	61	226	709	2309	6775	17747	43749				47593	0.269
		$\dot{V}$ (3):	15909	14071	12528	10101	7237	4024	1650	420	4				0	
		V (5):	0	5796	10027	15800	21532	27050	30624	32019					32087	
	300	D (6):	0	44	159	537	1494	4166	10478	24117					33687	0.161
		$\dot{V}$ (3):	47727	34077	25521	15762	8262	3105	822	71					0	
		V (5):	0	14136	20600	26691	30787	33526	34651						34753	
	1000	D (6):	0	114	369	1064	2529	6035	13437						21070	0.091
		$\dot{V}$ (2):	15909	6241	3284	1339	489	125	15						0	
		V (5):	0	23956	29627	33241	35085	36019							36162	
	3000	D (6):	0	230	624	1540	3271	7126							13080	0.053
		$\dot{V}$ (2):	47727	6498	2269	678	195	30							0	
		V (5):	0	31560	34768	36223	36821								36985	
	9000	D (7):	0	3537	8371	18637	37083								79003	0.031
		$\dot{V}$ (1):	14318	412	100	25	5								0	
		V (7):	0	290	579	1150	2132	4163	7939	14462	24841	35480	39802	41337	41793	
.80	.1	D (7):	0		1	3	11	45	175	656	2505	7995	14738	21965	33526	1.391
		$\dot{V}$ (6):	20513	20380	20248	19987	19538	18608	16872	13853	8970	3748	1429	458	0	
		V (6):	0	87	174	345	639	1246	2372	4306	7349	10399	11590	11982	12070	
	.3	D (7):	0	1	2	10	34	135	522	1959	7443	23602	43295	64289	92126	1.325
		$\dot{V}$ (6):	61538	61124	60712	59896	58494	55596	50212	40913	26071	10530	3806	1075	0	
		V (6):	0	290	578	1147	2122	4125	7801	13991	23363	32088	35065	35794	35862	
	1	D (6):	0		1	3	11	45	173	642	2402	7453	13464	19772	24478	1.185
		$\dot{V}$ (5):	20513	20355	20198	19889	19359	18271	16277	12921	7802	2810	835	133	0	
		V (6):	0	869	1730	3423	6303	12133	22531	39141	61924	79544	83588		83939	
	3	D (6):	0	1	2	10	34	133	505	1836	6612	19496	34073		46544	0.959
		$\dot{V}$ (5):	61538	60897	60263	59017	56907	52663	45184	33452	17594	4678	714		0	
		V (5):	0	288	571	1120	2029	3784	6644	10560	14678	16607			16697	
	10	D (6):	0	2	8	32	111	423	1547	5281	17241	45592			65299	0.666
		$\dot{V}$ (4):	20513	20105	19708	18943	17694	15350	11719	7106	2594	242			0	
		V (5):	0	853	1668	3189	5547	9594	15004	20524	24235				24822	
	30	D (6):	0	6	24	93	312	1129	3798	11531	32641				65051	0.435
		$\dot{V}$ (4):	61538	58697	56037	51202	44050	32749	19558	8281	1524				0	
		V (5):	0	2716	5086	9024	14120	20743	26829	30720					31823	
	100	D (6):	0	20	75	278	860	2754	7921	20371					50915	0.256
		$\dot{V}$ (3):	20513	17840	15650	12305	8522	4524	1762	418					0	
		V (5):	0	7202	12261	18922	25237	31069	34673	35976					36017	
	300	D (6):	0	54	194	645	1760	4812	11900	27053					35593	0.153
		$\dot{V}$ (3):	61538	42031	30491	18019	9051	3245	815	55					0	
		V (5):	0	16984	24234	30726	34938	37657	38709						38782	
	1000	D (6):	0	141	440	1235	2885	6784	14955						22077	0.086
		$\dot{V}$ (2):	20513	7263	3636	1418	500	123	13						0	
		V (5):	0	27759	33804	37438	39233	40117							40233	
	3000	D (6):	0	268	715	1736	3651	7891							13640	0.050
		$\dot{V}$ (2):	61538	7122	2340	678	192	27							0	
		V (5):	0	35709	38955	40364	40940								41077	
	9000	D (7):	0	4015	9374	20681	40924								82115	0.02
		$\dot{V}$ (1):	18462	428	99	24	5								0	
		V (7):	0	420	838	1665	3085	6019	11460	20815	35558	50433	56385	58504	59207	
1.00	.1	D (7):	0		1	5	16	62	240	900	3421	10863	19957	29685	47541	1.448
		$\dot{V}$ (6):	31250	31041	30833	30421	29714	28251	25530	20826	13312	5454	2063	679	0	
		V (6):	0	126	251	499	924	1801	3422	6188	10491	14723	16345	16876	17013	
	.3	D (6):	0			1	5	19	72	268	1015	3197	5842	8654	12941	1.374
		$\dot{V}$ (6):	93750	93091	92437	91141	88918	84333	75847	61310	38463	15169	5416	1571	0	
		V (6):	0	420	837	1660	3068	5953	11219	20000	33058	44873	48773	49711	49804	
	1	D (6):	0		1	5	16	62	236	876	3254	10002	17968	26300	33134	1.203
		$\dot{V}$ (5):	31250	30994	30740	30238	29381	27629	24443	19154	11289	3917	1133	185	0	
		V (5):	0	126	250	495	909	1743	3215	5520	8579	10830	11315		11352	
	3	D (6):	0	1	3	13	47	182	688	2482	8821	25618	44422		59773	0.950
		$\dot{V}$ (5):	93750	92669	91602	89512	85987	78958	66779	48217	24295	6047	837		0	
		V (5):	0	417	824	1612	2905	5365	9265	14384	19458	21628			21702	
	10	D (6):	0	3	11	44	151	573	2075	6959	22201	57530			78883	0.646
		$\dot{V}$ (4):	31250	30529	29830	28495	26343	22397	16526	9523	3219	244			0	
		V (5):	0	1230	2394	4540	7798	13202	20060	26600	30664				31195	
	30	D (6):	0	8	33	127	421	1499	4933	14586	40217				75037	0.416
		$\dot{V}$ (4):	93750	88601	83847	75368	63215	44977	25272	9954	1610				0	
		V (5):	0	3876	7170	12466	19001	27025	33893	37976					38982	
	100	D (6):	0	27	102	370	1124	3501	9784	24539					56771	0.243
		$\dot{V}$ (3):	31250	26410	22601	17060	11219	5553	2014	437					0	

TABLE 4.1—COMPUTED MOTION PARAMETERS FOR OBJECTS DISPLACED BY CLASSICAL BLAST WAVES (Continued)

P	A	T:	0	.002	.004	.008	.015	.030	.060	.120	.250	.500	.750	1.000	Final	T_{final}
1.00	300	V (5):	0	10033	16653	24913	32218	38567	42263	43476					43498	
		D (6):	0	72	254	827	2198	5839	14111	31574					38927	0.145
		V̇ (3):	93750	59448	40990	22619	10682	3599	846	39					0	
	1000	V (5):	0	22441	31088	38257	42633	45389	46370						46418	
		D (6):	0	182	551	1504	3435	7925	17252						23839	0.081
		V̇ (2):	31250	9401	4355	1595	543	126	10						0	
	3000	V (5):	0	34854	41589	45220	47022	47849							47935	
		D (6):	0	331	857	2038	4227	9043							14623	0.047
		V̇ (2):	93750	8471	2520	721	194	25							0	
	9000	V (5):	0	43453	46703	48152	48703								48810	
		D (7):	0	4754	10898	23754	46671								87711	0.027
		V̇ (1):	28125	467	109	25	5								0	
1.3	.1	V (7):	0	644	1283	2545	4706	9143	17279	31000	52023	72550	80561	83400	84435	
		D (7):	0		2	6	23	89	342	1272	4768	14907	27164	40221	68159	1.523
		V̇ (6):	50904	50500	50100	49312	47968	45231	40280	32103	19851	7861	2931	981	0	
	.3	V (6):	0	193	385	763	1410	2735	5153	9199	15302	21098	23258	23963	24163	
		D (6):	0			2	7	27	102	379	1411	4374	7924	11684	18340	1.435
		V̇ (5):	15271	15144	15017	14769	14345	13486	11940	9413	5699	2166	761	226	0	
	1	V (6):	0	643	1280	2536	4673	9018	16831	29538	47752	63543	68549	69768	69898	
		D (6):	0		2	6	23	88	336	1230	4492	13551	24115	35121	45333	1.230
		V̇ (5):	50904	50404	49910	48940	47297	43997	38182	29020	16374	5421	1540	261	0	
	3	V (5):	0	193	382	754	1381	2626	4774	8022	12117	14960	15538		15578	
		D (6):	0	1	5	19	67	259	970	3446	11967	33980	58322		78039	0.949
		V̇ (4):	15271	15057	14847	14438	13757	12428	10219	7064	3353	781	101		0	
	10	V (5):	0	637	1256	2443	4367	7936	13367	20085	26277	28703			28770	
		D (6):	0	4	16	63	215	807	2867	9372	28995	73370			97398	0.632
		V̇ (4):	50904	49455	48062	45435	41294	33999	23848	12837	3991	253			0	
	30	V (5):	0	1872	3618	6780	11439	18807	27541	35259	39647				40132	
		D (6):	0	12	47	180	588	2052	6556	18764	50225				88643	0.401
		V̇ (3):	15271	14232	13292	11664	9434	6324	3294	1194	170				0	
	100	V (5):	0	5816	10573	17897	26386	36110	43817	48061					48968	
		D (6):	0	38	143	510	1509	4547	12291	30002					64662	0.232
		V̇ (3):	50904	41285	34139	24405	15046	6869	2306	455					0	
	300	V (5):	0	14564	23417	33709	42203	49042	52783	53889					53899	
		D (6):	0	99	345	1085	2797	7203	16988	37403					43367	0.137
		V̇ (2):	15271	8748	5652	2880	1262	399	88	2					0	
	1000	V (5):	0	30518	40988	48842	53364	56088	56984						57012	
		D (6):	0	240	705	1863	4153	9398	20201						26147	0.076
		V̇ (2):	50904	12461	5223	1787	583	128	8						0	
	3000	V (5):	0	44930	52201	56004	57781	58541							58603	
		D (6):	0	416	1044	2429	4966	10518							15899	0.044
		V̇ (1):	15271	1017	285	76	20	2							0	
	9000	V (5):	0	54258	57460	58925	59432								59514	
		D (7):	0	5716	12862	27692	54027								94835	0.026
		V̇ (1):	45813	504	117	25	4								0	
1.7	.1	V (6):	0	97	193	382	705	1364	2561	4546	7516	10345	11436	11827	11989	
		D (7):	0	1	2	9	31	122	469	1731	6412	19799	35857	52921	97502	1.638
		V̇ (6):	83046	82300	81562	80112	77653	72698	63917	49918	30033	11642	4342	1502	0	
	.3	V (6):	0	290	577	1144	2110	4076	7628	13462	22037	29966	32887	33854	34170	
		D (6):	0		1	3	9	37	140	515	1893	5791	10424	15318	25785	1.525
		V̇ (5):	24914	24677	24443	23984	23206	21645	18899	14575	8565	3181	1119	348	0	
	1	V (6):	0	966	1921	3800	6986	13412	24807	42926	68075	89200	95776	97464	97673	
		D (6):	0	1	2	9	31	121	459	1664	5981	17764	31384	45548	61411	1.278
		V̇ (5):	83046	82106	81179	79366	76320	70283	59924	44304	24092	7753	2232	419	0	
	3	V (5):	0	289	573	1128	2056	3880	6958	11460	16885	20496	21221		21279	
		D (5):	0		1	3	9	35	132	460	1565	4361	7427		10100	0.965
		V̇ (4):	24914	24503	24101	23324	22044	19599	15682	10413	4703	1062	145		0	
	10	V (5):	0	955	1877	3630	6431	11499	18903	27570	35083	37881			37957	
		D (5):	0	1	2	9	29	109	380	1213	3652	9067			11948	0.630
		V̇ (4):	83046	80201	77493	72452	64688	51545	34415	17426	5090	305			0	
	30	V (5):	0	2792	5357	9908	16414	26200	37099	46108	50917				51407	
		D (5):	0	2	6	24	79	269	836	2324	6071				10426	0.395
		V̇ (3):	24914	22860	21046	17997	14017	8867	4309	1461	193				0	
	100	V (5):	0	8537	15235	25108	35862	47424	55988	60447					61316	
		D (6):	0	52	192	672	1940	5667	14882	35525					73475	0.226
		V̇ (3):	83046	64348	51304	34681	20100	8534	2695	498					0	
	300	V (5):	0	20626	32179	44690	54292	61727	65583	66639					66643	
		D (6):	0	134	449	1367	3424	8581	19838	43129					48278	0.133
		V̇ (2):	24914	12805	7748	3670	1526	454	95	2					0	
	1000	V (5):	0	40614	53232	61542	66335	69064	69913						69930	
		D (6):	0	305	866	2225	4863	10833	23058						28706	0.074
		V̇ (2):	83046	16580	6232	2076	643	137	7						0	
	3000	V (5):	0	57276	64994	69046	70809	71537							71587	
		D (6):	0	503	1230	2810	5681	11938							17324	0.043
		V̇ (1):	24914	1224	333	83	21	2							0	
	9000	V (5):	0	67375	70525	71957	72458								72529	
		D (6):	0	666	1476	3148	6108								10285	0.025
		V̇ (1):	74741	543	126	27	4								0	

Chapter 5

INTERPRETATION OF RESULTS

5.1 GENERAL REMARKS

The motion parameters of secondary missiles computed in the present study can be used in many different ways. The purpose of this chapter is to point out a few analytical techniques that have been found useful. Although the treatment is not exhaustive, such practical subjects as weapon scaling, acceleration coefficients, and interpolation techniques are discussed. In addition, samples of computed missile data are shown in graphic form.

5.2 ACCELERATION COEFFICIENTS FOR VARIOUS OBJECTS

Acceleration coefficient has been defined as the product of the area presented to the wind by an object and its drag coefficient divided by its mass. To vivify the meaning of the computed results, it is necessary to relate values of acceleration coefficient to real objects. For this purpose Table 5.1 (based on Refs. 1–3) was prepared.

In regard to the acceleration coefficient for man, it is evident from these data that position with respect to the wind is quite important. Change of position during translation, as well as surface-friction effects, serves to complicate any attempt at an exact analysis. With respect to this problem, it is useful to note the results of an experiment reported by Taborelli et al.[4] in which anthropometric dummies, weighing 169 lb dressed and having a height of 5 ft 9 in., were used in connection with full-scale weapons tests. In one instance a dummy was placed on a concrete ramp standing with its back to the oncoming blast wave. The blast parameters at this location were: maximum overpressure 5.3 psi, ambient pressure 13.3 psi, duration of positive pressure 0.964 sec, and the velocity of sound in the ambient air 1120 ft/sec. Partial results of the motion picture analysis shown in Fig. 5.1 indicate that the dummy was accelerated to 21.4 ft/sec in 0.5 sec after having been displaced about 8 ft. By this time the dummy's position, which was initially vertical, had become horizontal with the head toward the oncoming blast wave (see chart at top of Fig. 5.1). Also shown on this figure are predicted velocity-time histories for various values of acceleration coefficient. It is interesting to note that early in the displacement record, the dummy's velocity corresponded closely with that predicted for a man standing broadside to the wind ($\alpha = 0.052$ ft^2/lb, see Table 5.1). At later times, because of rotation, the dummy's increase in velocity with time corresponded more closely with that predicted for a prone man aligned with the wind (see lower curve on Fig. 5.1). It should be noted that the record obtained for the dummy was terminated because dust obscured the test area; therefore, the latter part of the record was less accurately determined than the initial portion. There was some indication that the dummy's velocity was increasing slightly at the termination of the record. However, if 21.4 ft/sec is assumed to have been the maximum velocity attained, then it is possible to determine an acceleration coefficient that would produce a predicted maximum velocity of the same value (21.4 ft/sec) under the same blast conditions. The effective acceleration coefficient so determined had a value of 0.0268 ft^2/lb. This is remarkably close to 0.03 ft^2/lb computed

TABLE 5.1—TYPICAL ACCELERATION COEFFICIENTS (α)

	α, ft^2/lb	Reference
168-lb man:		
Standing facing wind	0.052	1
Standing sidewise to wind	0.022	1
Crouching facing wind	0.021	1
Crouching sidewise to wind	0.017	1
Prone aligned with wind	0.0063	1
Prone perpendicular to wind	0.022	1
Average value for tumbling man in straight, rigid position	0.030	2
21-g mice, maximum presented area	0.38	2
180-g rats, maximum presented area	0.19	2
530-g guinea pigs, maximum presented area	0.15	2
2100-g rabbits, maximum presented area	0.079	2
Typical stones:		
0.1 g	0.67	2
1.0 g	0.32	2
10.0 g	0.15	2
Window-glass fragments, $\frac{1}{8}$ in. thick:		
0.1 g, all orientations	0.78	2
1.0 g, edgewise and broadside to wind	0.48–0.57	2
10.0 g, edgewise and broadside to wind	0.34–0.72	2
Steel spheres:		
$\frac{1}{8}$ in. diameter	0.139	3
$\frac{1}{4}$ in. diameter	0.0696	3
$\frac{7}{16}$ in. diameter	0.0398	3
$\frac{1}{2}$ in. diameter	0.0348	3
$\frac{9}{16}$ in. diameter	0.0310	3

for a tumbling man in a straight, rigid position (see Table 5.1). Using the latter value, a predicted maximum velocity of 23.4 ft/sec was obtained in a displacement of 19.5 ft (see plotted point in Figure 5.1). The total displacement of the dummy, measured after the event, was 21.9 ft. This figure included, of course, the distance required for the dummy to come to a stop after maximum velocity had been reached, and therefore it cannot be compared directly with displacement predicted at the time of maximum velocity.

Other field studies[5,6] have been made to evaluate the velocities of glass-fragment missiles originating from windows facing the oncoming blast wave (the window frames were mounted in the open and in houses). It was found in the case of the house-mounted windows that a considerable portion of the missile sample from each window had velocities higher than could be explained if acceleration coefficients noted in Table 5.1 were used in applying the results of the present study to the blast situations encountered in the field operations. However, if one computed on the basis of a reflected blast wave, the higher missile velocities were satisfactorily explained. Thus, it appears that the somewhat complicated hydrodynamic phenomena occurring when a blast wave enters a house by way of a window or windows produces missile results equivalent to a shock overpressure more than twice as great as the overpressure actually incident upon the house.

Acceleration coefficients for steel spheres have been included in Table 5.1 for comparative purposes. For instance, the alphas for a tumbling man and a steel sphere $\frac{9}{16}$ in. in diameter are about the same. Similarly, $\frac{1}{8}$ in. steel spheres and guinea pigs are approximately equivalent in so far as translation by blast waves is concerned. Thus, in theory, an "equivalent" sphere can be found for any irregular object. This concept has been used in weapon-effects tests[4,6] taking advantage of the fact that velocity can be experimentally determined more readily for a sphere than for the object it represents.

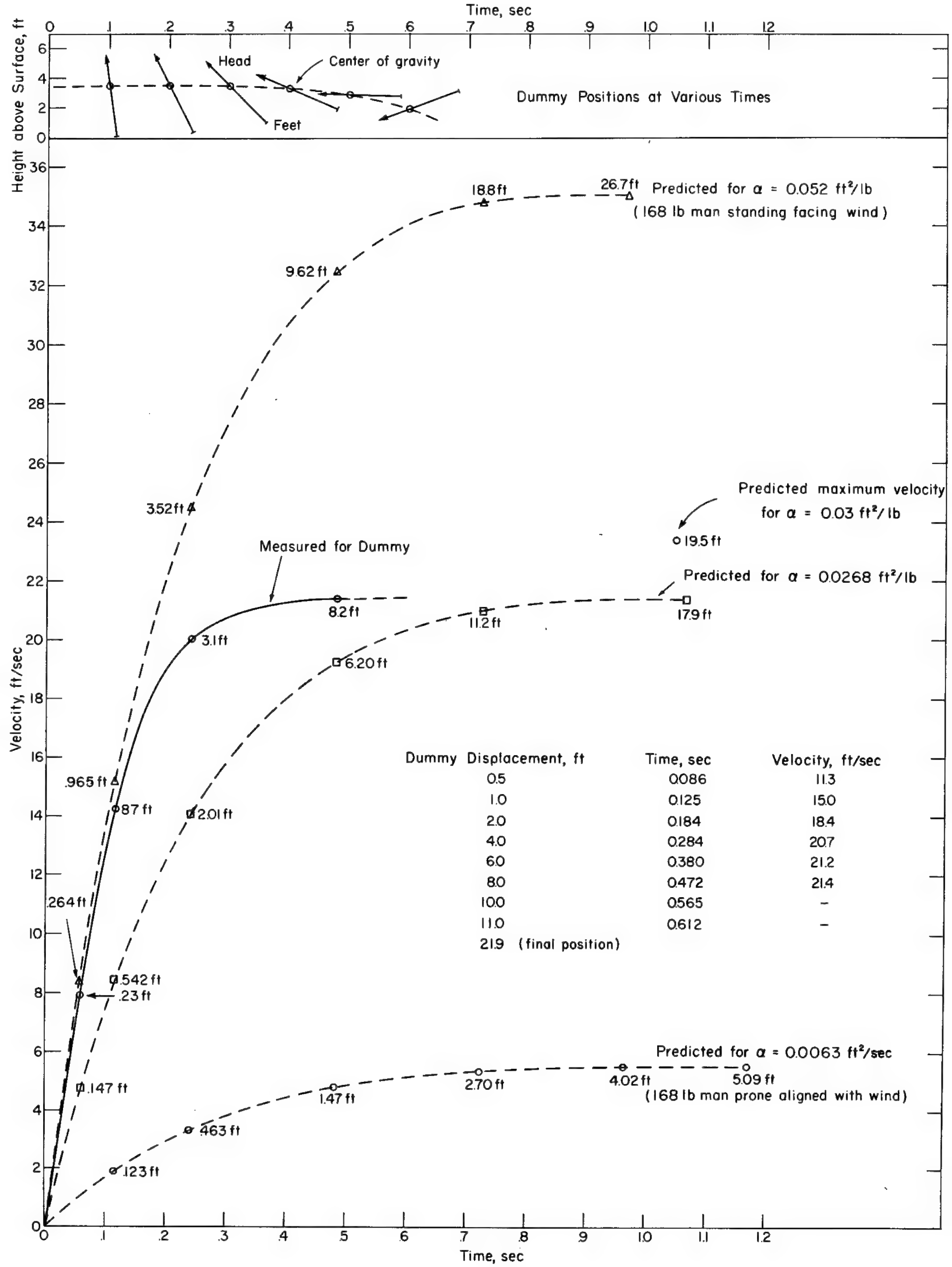

Fig. 5.1—Anthropometric dummy translation history, obtained from full-scale weapon test,[4] compared with that predicted using various values of acceleration coefficient (see Table 5.1) and the computed data in Table 4.1. Numbers adjacent to plotted points indicate measured or computed displacements. Blast parameters: p_s = 5.3 psi, p_0 = 13.3 psi, t_p^+ = 0.964 sec, c_0 = 1120 ft/sec.

5.3 WEAPON YIELD AS A BLAST PARAMETER

Although the motion parameters were evaluated without regard to yield, introduction of the latter at this point is both interesting and useful. Employing the well-known weapon-scaling law[7,8] applying to given values of shock overpressures, the following relation can be written:

$$\frac{t_p^+}{(t_p^+)_1} = \frac{t_u^+}{(t_u^+)_1} = \left[\frac{W(p_0)_1}{W_1 p_0}\right]^{1/3} \frac{(c_0)_1}{c_0} \tag{5.1}$$

Quantities marked with the subscript "1" are considered to be constant and to have reference or "standard" values. The parameters not so marked can take any set of appropriate values.

The next step is taken from the definitions of dimensionless acceleration coefficient (A) and displacement (D). The subscript marking is similar to that for Eq. 5.1.

$$\left(\frac{\alpha p_0 t_u^+}{c_0}\right)_1 = \frac{\alpha p_0 t_u^+}{c_0} \tag{5.2}$$

$$\frac{d}{t_u^+ c_0} = \left(\frac{d}{t_u^+ c_0}\right)_1 \tag{5.3}$$

Eliminating $t_u^+/(t_u^+)_1$ between Eq. 5.1 and Eqs. 5.2 and 5.3, in turn, the following is obtained:

$$\alpha_1 = \alpha \left[\frac{(c_0)_1}{c_0}\right]^2 \left[\frac{p_0}{(p_0)_1}\right]^{2/3} \left(\frac{W}{W_1}\right)^{1/3} \tag{5.4}$$

$$d = d_1 \left[\frac{W}{W_1} \frac{(p_0)_1}{p_0}\right]^{1/3} \tag{5.5}$$

Thus, weapon yield replaces duration as parameter. The significance of this transformation will be demonstrated in Sec. 5.4.

5.4 MAXIMUM VELOCITY AND CORRESPONDING DISPLACEMENT

Data in Table 4.1, along with Eq. 2.24, were used to prepare Fig. 5.2, which shows the maximum missile velocity as a function of acceleration coefficient and shock overpressure. The tabulated data were made dimensional for a 1-kt burst where the ambient pressure and speed of sound were 14.7 psi and 1117 ft/sec, respectively. By use of the transformation equation, Eq. 5.4, and the definition of dimensionless velocity, the data on this chart can be made to apply to other conditions where W, p_0, and c_0 may be different from those used in the construction of the chart.

Consider the translation of a man whose average alpha is 0.03 ft^2/lb. For a 1-kt burst at a range where the shock overpressure is 1 atm, his maximum velocity is predicted to be 37 ft/sec (see Fig. 5.2). If the yield were 1000 kt, however, the adjusted alpha, α_1, becomes 0.3. Entering this value for alpha on the same chart, again at the 1-atm curve, a maximum velocity of 195 ft/sec is obtained.

Figure 5.3 shows, for a 1-kt burst, displacement at maximum velocity as a function of alpha and shock overpressure, prepared for the same ambient conditions used for Fig. 5.2. Continuing the example used above, the man would be displaced 9 ft when maximum velocity was reached if the yield were 1 kt. However, if it were 1000 kt, his displacement would be $28 \times 1000^{1/3} = 280$ ft (see Eqs. 5.4 and 5.5).

Figures 5.4 to 5.7 are similar to those described above except that the yields are 20 kt and 1000 kt (1 Mt). The charts prepared for 1 kt could be used for all yields, except for limitations in the range of the abscissa.

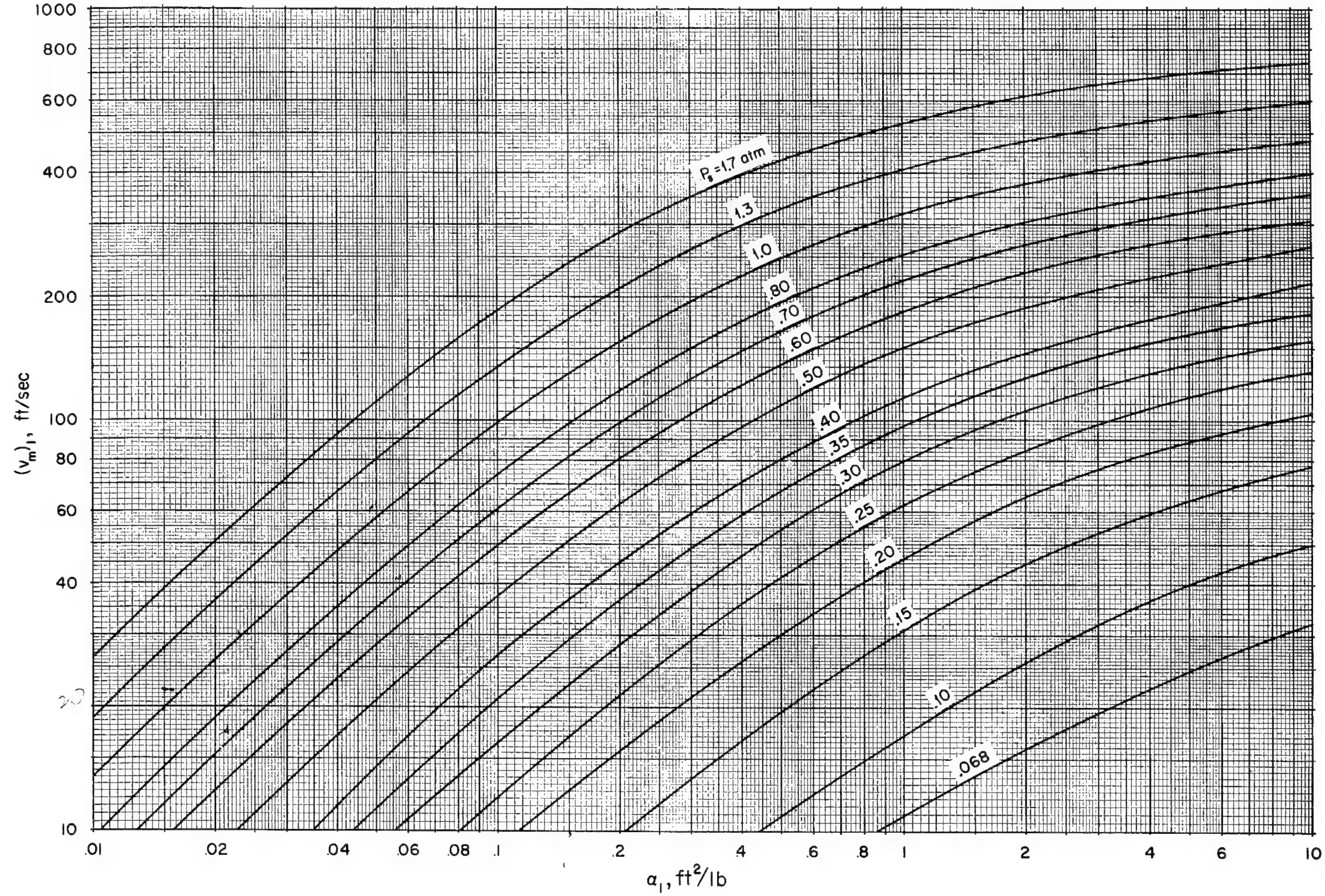

Fig. 5.2—Predicted maximum velocity as a function of acceleration coefficient (α) and shock overpressure computed for W = 1 kt, p_0 = 14.7 psi, and c_0 = 1117 ft/sec. For other conditions, use:

$$\alpha_1 = \alpha\left(\frac{1117}{c_0}\right)^2 \left(\frac{p_0}{14.7}\right)^{2/3} W^{1/3} \qquad v_m = (v_m)_1\left(\frac{c_0}{1117}\right)$$

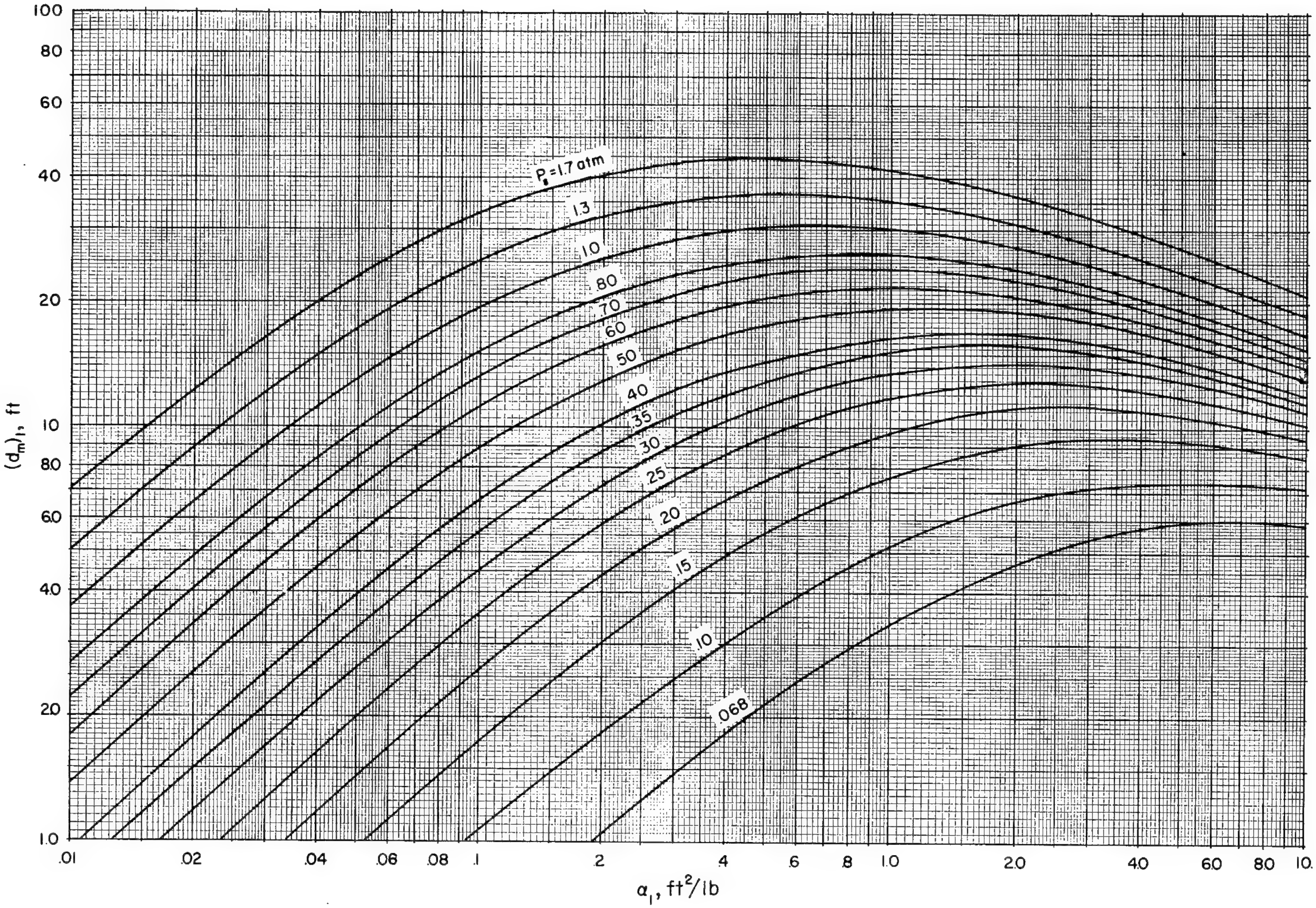

Fig. 5.3—Predicted displacement at maximum velocity as a function of acceleration coefficient (α) and shock overpressure computed for W = 1 kt, p_0 = 14.7 psi, and c_0 = 1117 ft/sec. For other conditions, use:

$$\alpha_1 = \alpha\left(\frac{1117}{c_0}\right)^2 \left(\frac{p_0}{14.7}\right)^{2/3} W^{1/3} \qquad d_m = (d_m)_1 \left(\frac{14.7\ W}{p_0}\right)^{1/3}$$

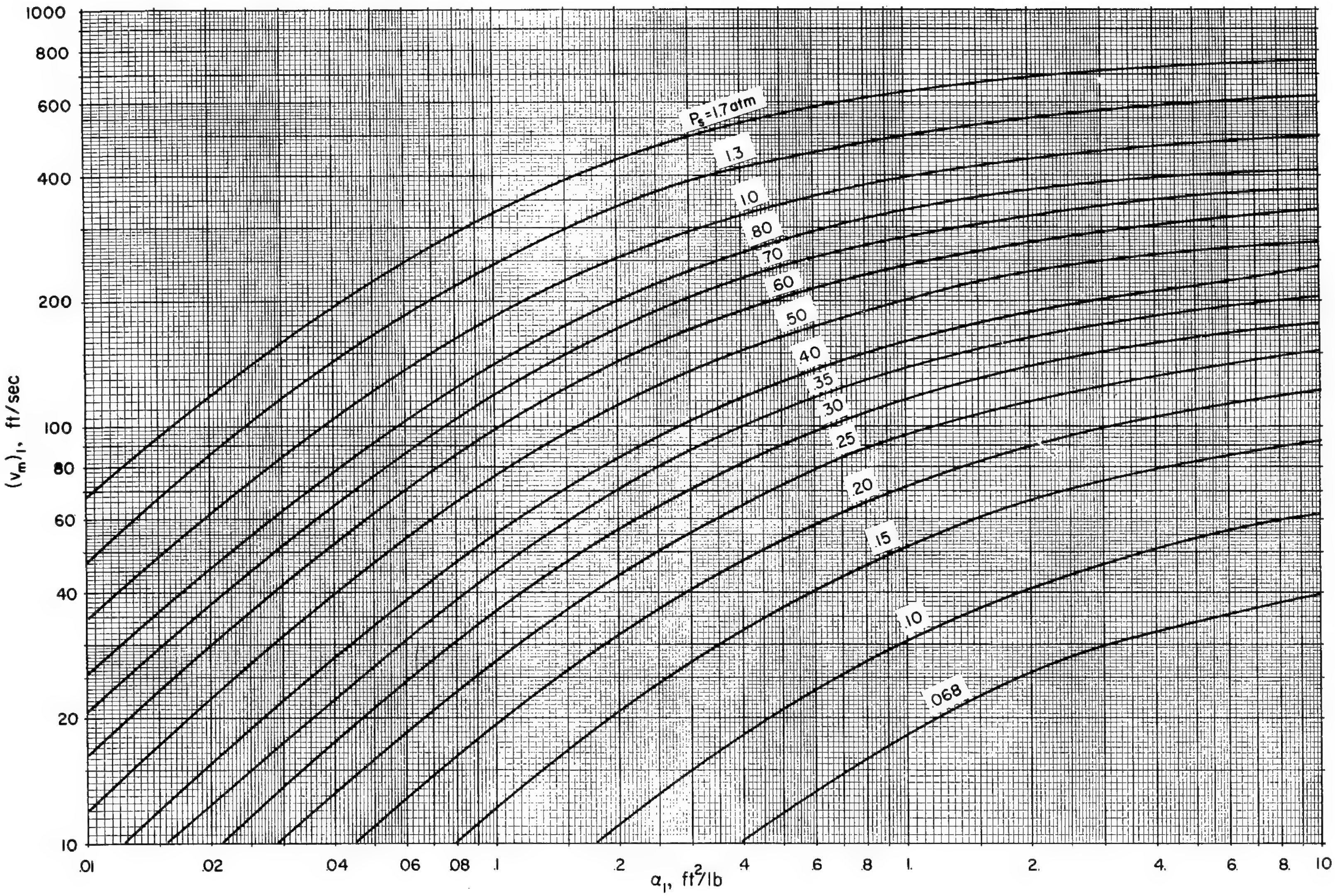

Fig. 5.4—Predicted maximum velocity as a function of acceleration coefficient (α) and shock overpressure computed for W = 20 kt, p_0 = 14.7 psi, and c_0 = 1117 ft/sec. For other conditions, use:

$$\alpha_1 = \alpha\left(\frac{1117}{c_0}\right)^2\left(\frac{p_0}{14.7}\right)^{2/3}\left(\frac{W}{20}\right)^{1/3} \qquad v_m = (v_m)_1\,\frac{c_0}{1117}$$

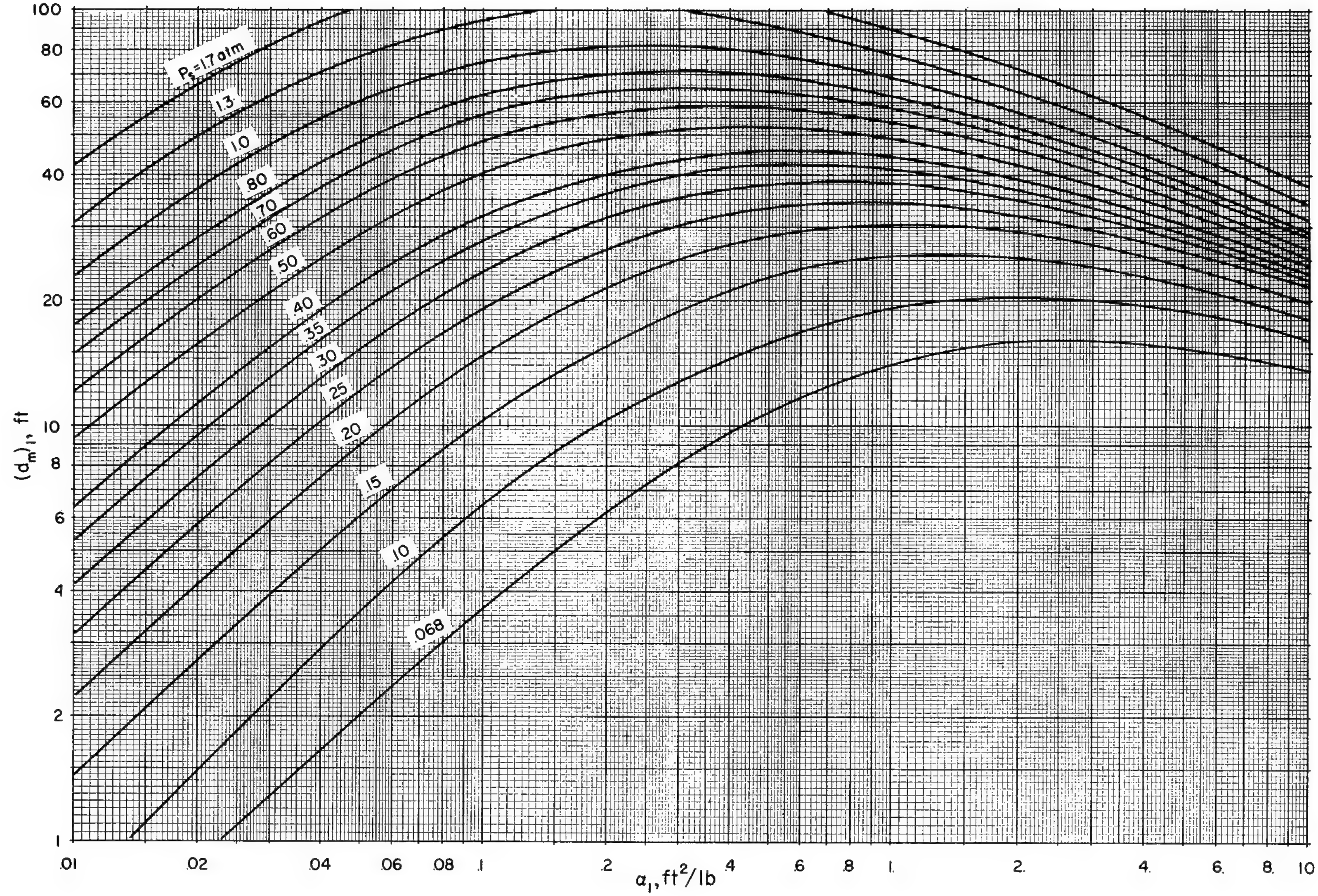

Fig. 5.5—Predicted displacement at maximum velocity as a function of acceleration coefficient (α) and shock overpressure computed for W = 20 kt, p_0 = 14.7 psi, and c_0 = 1117 ft/sec. For other conditions, use:

$$\alpha_1 = \alpha\left(\frac{1117}{c_0}\right)^2\left(\frac{p_0}{14.7}\right)^{2/3}\left(\frac{W}{20}\right)^{1/3} \qquad d_m = (d_m)_1\left(\frac{14.7\,W}{p_0 20}\right)^{1/3}$$

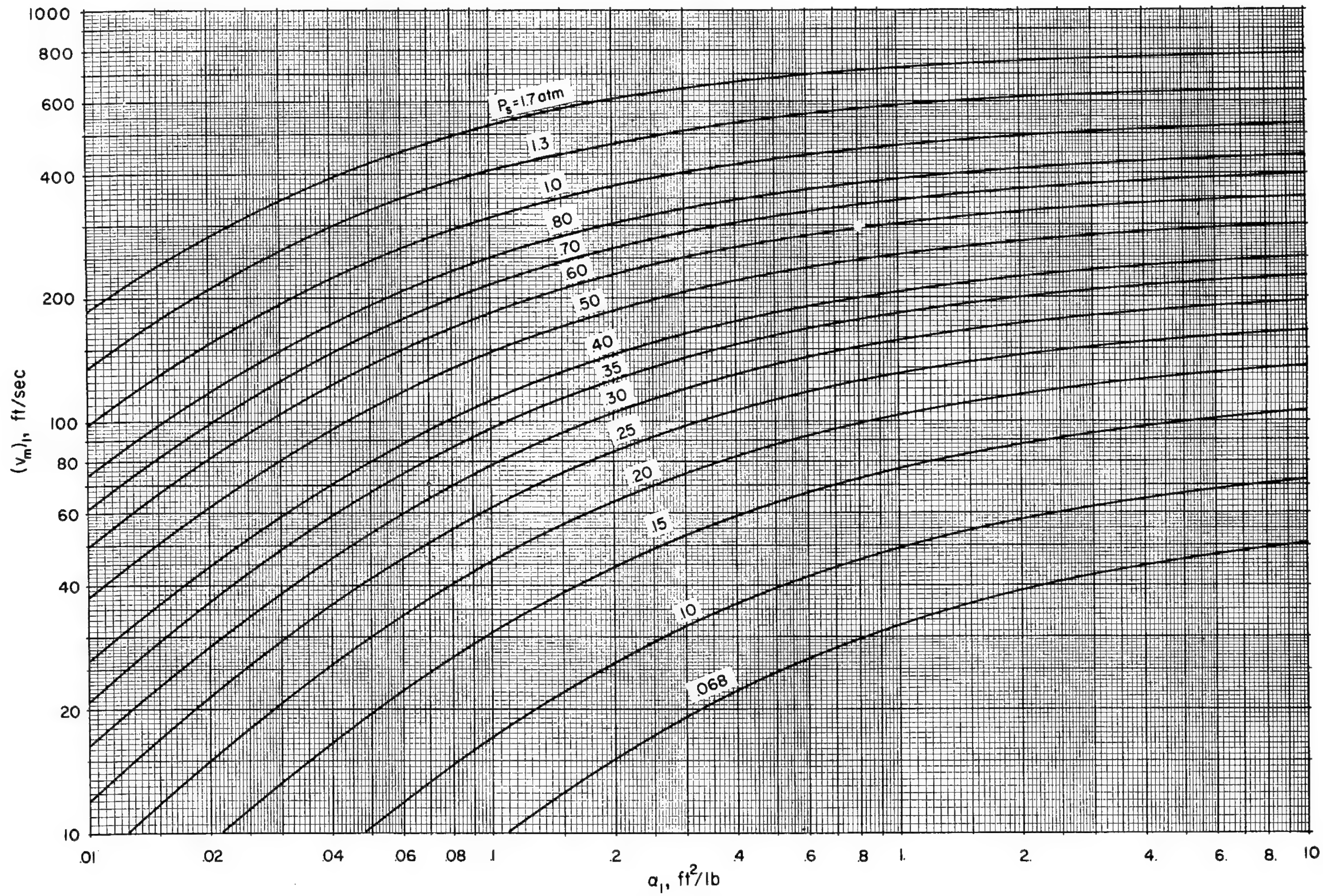

Fig. 5.6—Predicted maximum velocity as a function of acceleration coefficient (α) and shock overpressure computed for W = 1000 kt (1 Mt), p_0 = 14.7 psi, and c_0 = 1117 ft/sec. For other conditions, use:

$$\alpha_1 = \alpha\left(\frac{1117}{c_0}\right)^2 \left(\frac{p_0}{14.7}\right)^{2/3} \left(\frac{W}{1000}\right)^{1/3} \qquad v_m = (v_m)_1 \frac{c_0}{1117}$$

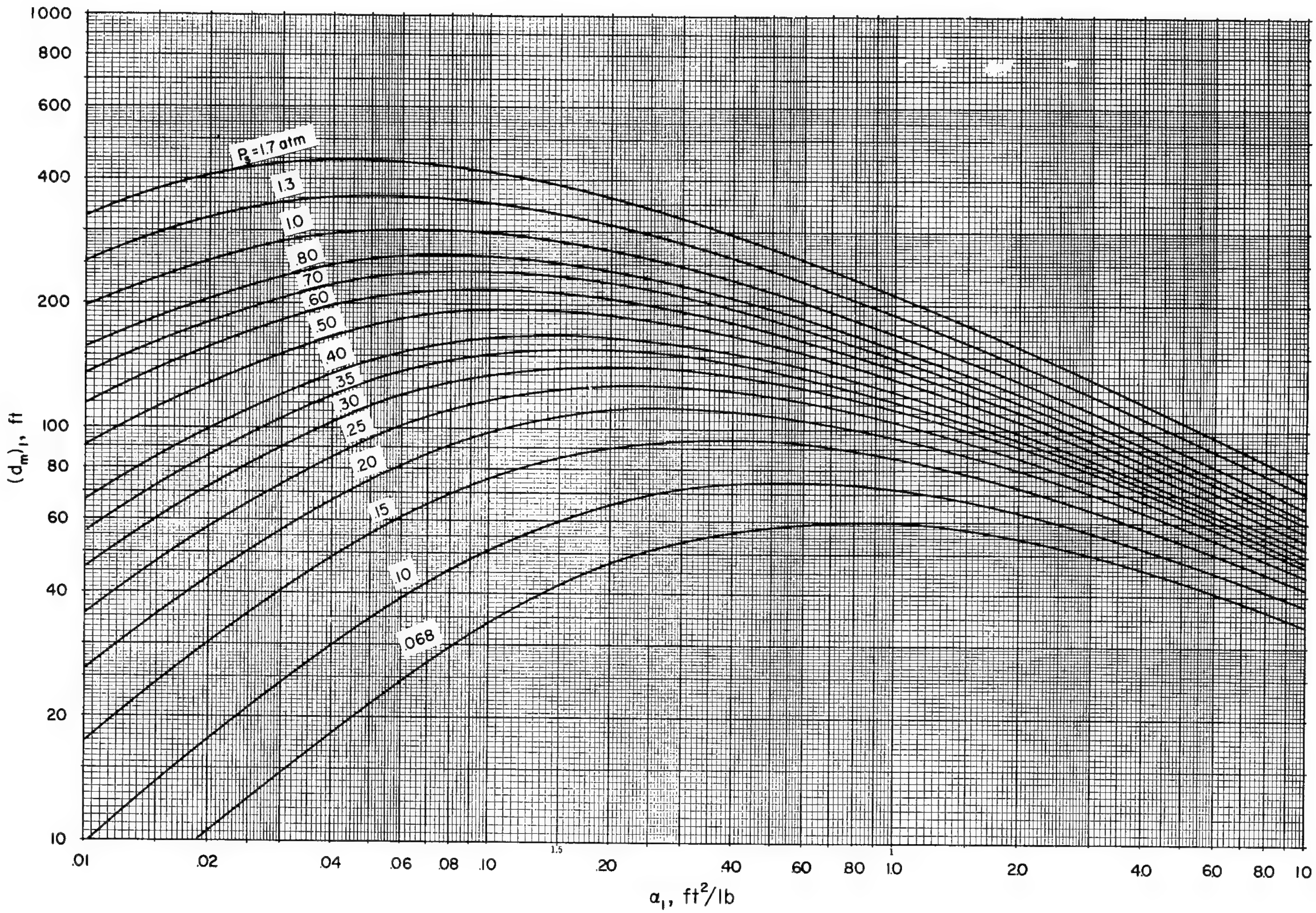

Fig. 5.7—Predicted displacement at maximum velocity as a function of acceleration coefficient (α) and shock overpressure computed for W = 1000 kt (1 Mt), p_0 = 14.7 psi, and c_0 = 1117 ft/sec. For other conditions, use:

$$d_m = (d_m)_1 \left(\frac{14.7\ W}{p_0 1000}\right)^{1/3} \qquad \alpha_1 = \alpha\left(\frac{1117}{c_0}\right)^2 \left(\frac{p_0}{14.7}\right)^{2/3} \left(\frac{W}{1000}\right)^{1/3}$$

5.5 ESTIMATION OF MAXIMUM VELOCITY FROM TOTAL DISPLACEMENT

Estimation of maximum velocity from total displacement can perhaps be described best by illustration. Suppose an object of unknown alpha were exposed to blast winds from a 1-Mt explosion at a location where the ambient pressure and speed of sound were 14.7 psi and 1117 ft/sec, respectively, and the shock overpressure was 0.35 atm (5.14 psi). After the explosion assume a total displacement of 100 ft was measured. This measurement includes, of course, the distance traveled by the object in stopping after maximum velocity had been reached. By use of the plotted data shown in Fig. 5.7, we can only say that the effective alpha must have been less than 0.0265. Then, referring to Fig. 5.6, it is determined that for an alpha less than 0.0265 under these blast conditions, the maximum velocity must have been less than 45 ft/sec.

The largest source of error in the above estimation, no doubt, embodies the use of total displacement as the displacement at the time of maximum velocity, i.e., "overshoot" was neglected. By means of simple experiments, the amount of overshoot, or stopping distance, could be determined as a function of initial velocity. Inclusion of this factor in the estimation procedure would result in a smaller but more accurate value for estimated maximum velocity.

Assuming that the overshoot is known, what are the assumptions involved in estimating maximum velocity from displacement? Essentially, it is assumed that the velocity-time history of an object is determined by the fact that it traveled a known distance in a known time. Mathematically, any number of velocity-time curves could satisfy the known distance-time values; however, the most likely one is assumed, in the above procedure, to be of the form of computed secondary-missile velocity vs. time for a classical blast wave. It is interesting to note that no previous knowledge of alpha is necessary and that an "effective" value is automatically obtained by the analytical procedure. Effective alpha could be modified in the real blast situation by such extraneous influences as ground friction or shielding without seriously affecting the accuracy of maximum velocity determined by displacement. However, if the missile were in the air at a considerable height at the time of maximum velocity and if the latter were fairly high, the estimate of overshoot could be seriously affected.

5.6 COMPUTED VELOCITY AND DISPLACEMENT FOR PARTICULAR OBJECTS

5.6.1 Interpolation of Alpha and Overpressure

Application of the computed motion parameters to specific objects and blast situations makes it necessary to interpolate between the values of alpha and/or shock overpressure for which computations were made. It has been found that linear interpolation produces results sufficiently accurate for most purposes. Graphic interpolation has also been found to produce satisfactory results. Charts prepared by such procedures will be presented later in this section.

5.6.2 Velocity and Displacement Predicted for Man and for Glass Fragments

Figure 5.8 was prepared, primarily, to illustrate the effect of yield on the velocity and displacement predicted for a tumbling man and 10-g fragments of glass arising from a window in a house (see Table 5.1 α values). The predictions apply to a shock overpressure of 5.14 psi, ambient pressure of 14.7 psi ($P = 0.35$ atm), and speed of sound of 1117 ft/sec. Also shown on Fig. 5.8 are the ranges from Ground Zero as a function of weapon yield where the stated shock overpressure could be expected to occur for a surface burst and a "typical" air burst.[7]

For illustrative purposes, the steps taken in the preparation of Fig. 5.8 are outlined. Velocity-displacement relations were sought for six yields from 1 kt to 20 Mt. For each yield, wind durations were computed for $P = 0.35$, $p_0 = 14.7$ psi, and $c_0 = 1117$ ft/sec, using Eq. 2.24 and Fig. 2.2. Dimensionless alpha, A, was then computed for each of the yield values used. The next step was to obtain velocity-displacement data from Table 4.1 for $P = 0.35$. For each of the times (T) listed in this table, corresponding values of velocity and displacement were computed by linear interpolation for the exact value of dimensionless alpha applicable to the yield being processed. Then velocity was plotted as a function of displacement for each of the

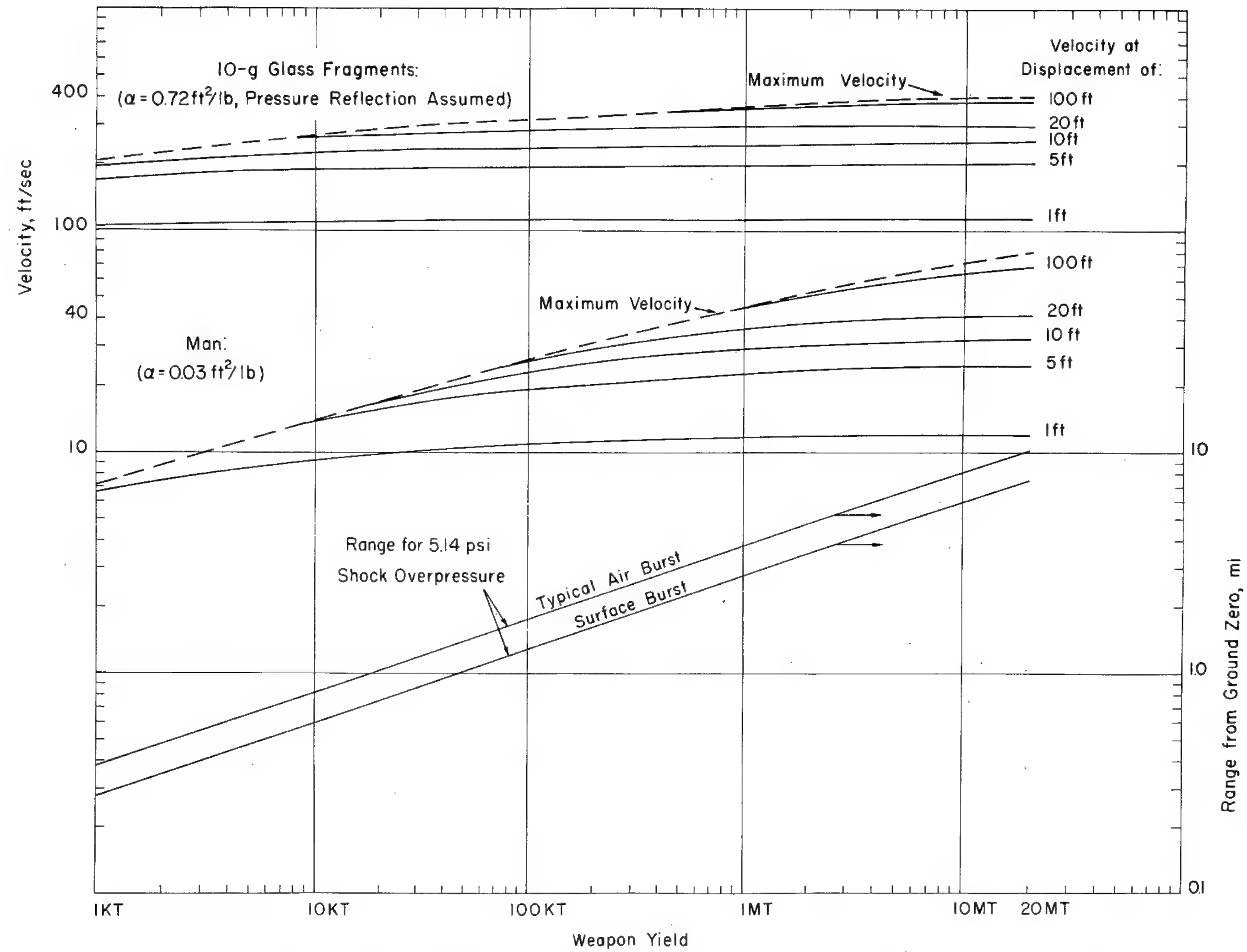

Fig. 5.8 — Relation between velocity and displacement as a function of weapon yield computed for 10-g glass fragments and man, where $p_s = 5.14$, $p_0 = 14.7$ psi, and $c_0 = 1117$ ft/sec. Range from Ground Zero where predicted data apply is shown as a function of weapon yield.

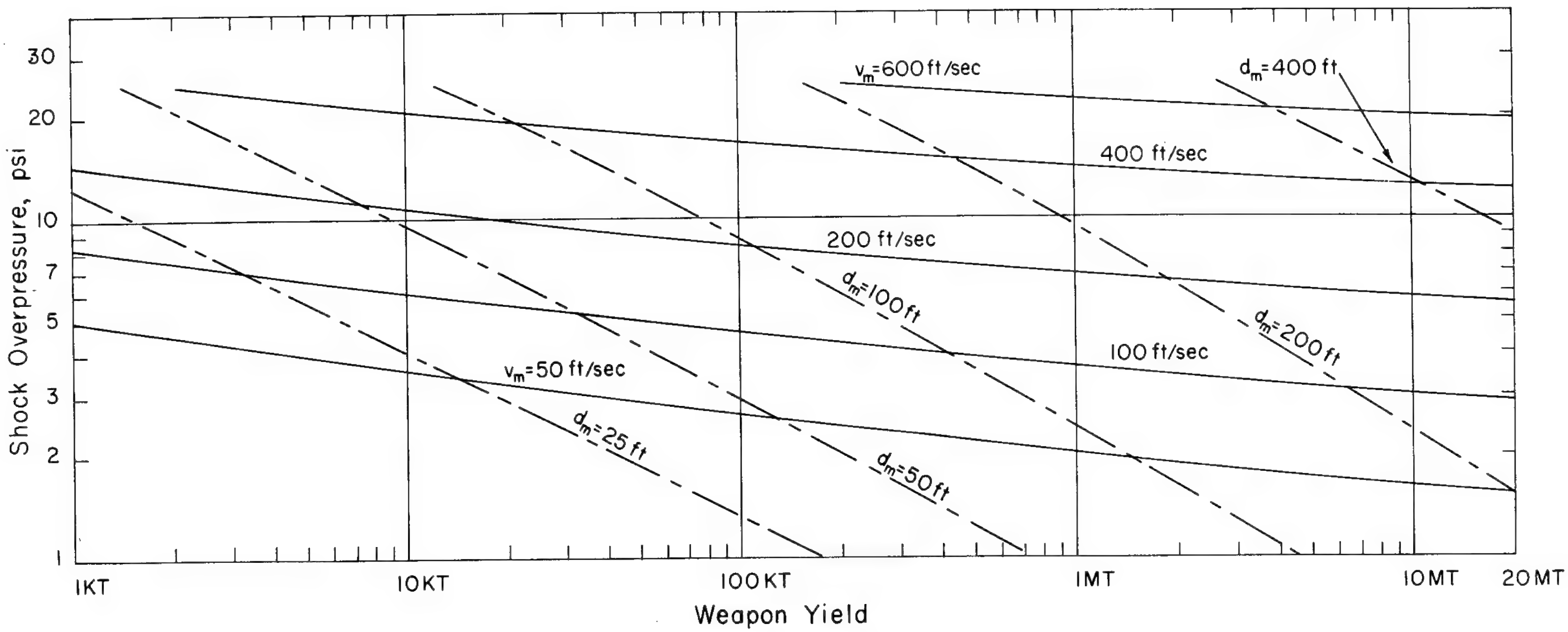

Fig. 5.9—Relation between shock overpressure and yield for various values of maximum velocity and displacement at maximum velocity computed for 1-g stones, where α = 0.32 ft^2/lb, p_0 = 14.7 psi, c_0 = 1117 ft/sec, v_m = computed maximum velocity, and d_m = displacement at maximum velocity.

six yields. Velocities were obtained from these plots at given displacement intervals until maximum velocity was reached. These data, along with the computed maximum velocities, were then used to plot the curves appearing in Fig. 5.8.

The procedure described above applies strictly to the treatment of the data for man. For the 10-g window-glass fragment study, it was assumed that the incident shock overpressure of 0.35 atm was reflected to 0.80 atm (see Sec. 5.2).

The plotted data appearing in Fig. 5.8 indicate that the velocity predicted for man is much more yield dependent than that for glass fragments. The reason for this is that the window glass having a higher alpha reaches wind velocity in a shorter time than does the man and therefore utilizes less of the longer duration produced by higher yield.

It is interesting to note that, for all yields, in only 1 ft of travel the glass fragments have already attained velocities greater than 100 ft/sec. Similarly, for all yields greater than 20 kt, man is predicted to be propelled at more than 10 ft/sec in just 1 ft of travel.

5.6.3 Predicted Maximum Velocities and Corresponding Displacements for 1-g Stones

The purpose of this analysis was to study the interplay of the effects of shock overpressure and weapon yield on the velocity and displacement of 1-g stones. The results, shown in Fig. 5.9, were plotted so that corresponding values of shock overpressure and weapon yield could be obtained for the plotted values of maximum velocity and displacement at maximum velocity. Data for this chart were scaled from those presented in Figs. 5.2 and 5.3.

An interesting concept to be derived from this analysis is that of "equivalent" shock overpressures; e.g., a 15-psi blast wave produced by a 1-kt burst is equivalent to a 5.7-psi wave from a 20-Mt burst in that both are predicted to propel 1-g stones at maximum velocities of 200 ft/sec. It should be pointed out, however, that the distances required to achieve maximum velocity are quite different. For the 1-kt burst the required distance is about 30 ft; whereas, for the 20-Mt burst it is about 300 ft.

From the data plotted in Fig. 5.9, it can be concluded that both velocity and displacement increase with pressure and yield; however, missile velocity is more sensitive to pressure (wind-velocity dependence) than is displacement; and, conversely, displacement is more sensitive to yield (duration effect) than is velocity.

REFERENCES

1. Thomas J. Schmitt, Wind-Tunnel Investigation of Air Loads on Human Beings, Report 892 (Aero 858), The David W. Taylor Model Basin Aerodynamics Laboratory, Washington, D. C., January 1954.
2. E. Royce Fletcher et al., Determination of Aerodynamic Drag Parameters of Small Irregular Objects by Means of Drop Tests, Civil Effects Test Operations, Report CEX-59.14 (in preparation).
3. Sighard F. Hoerner, author and publisher, *Fluid-Dynamic Drag*, Chap. III, pp. 3-8, Midland Park, N. J., 1958.
4. R. V. Taborelli, I. G. Bowen, and E. R. Fletcher, Tertiary Effects of Blast—Displacement, Operation Plumbbob Report, WT-1469, May 22, 1959.
5. I. G. Bowen, A. F. Strehler, and Mead B. Wetherbe, Distribution and Density of Missiles from Nuclear Explosions, Operation Teapot Report, WT-1168, March 1956.
6. I. G. Bowen et al., Secondary Missiles Generated by Nuclear-produced Blast Waves, Operation Plumbbob Report, WT-1468 (in preparation).
7. Samuel Glasstone (Ed.), *The Effects of Nuclear Weapons*, Superintendent of Documents, U. S. Government Printing Office, Washington, D. C., June 1957.
8. Harold L. Brode, Point Source Explosion in Air, Report AECU-3517, The Rand Corporation, Dec. 3, 1956.

Chapter 6

DISCUSSION

Although this study was intended to further the understanding of the secondary and tertiary effects of blast on a biological subject, the results are equally applicable to certain other investigative efforts, e.g., studies of physical damage resulting from secondary missiles or displacement. The model that was constructed to describe the motion of objects displaced by the blast wave requires no knowledge of the object displaced except its area presented to the wind, mass, and drag coefficient, all of which are assumed to be constant throughout the duration of the blast wave. In addition, the model requires that other forces which may be present, such as gravity and friction due to the object's moving over a surface, be negligible in comparison with those due to blast winds.

Thus, like most models, certain simplifying assumptions were made (see Sec. 1.3) in the interest of feasibility, simplicity, and uniformity. The determination of whether or not the results so computed apply with sufficient accuracy to particular situations is the subject of other investigations; in particular, those conducted in connection with full-scale nuclear weapons tests, the results of which[1] will be published soon. These field studies included the measurement of velocities for stones and spheres placed in open areas and also for fragments of glass from windows mounted in houses and in open areas. Experiments were conducted in locations where the incident blast wave varied from classical to nonclassical types. One experiment was conducted inside a shelter with an open entryway making use of steel spheres to estimate the velocities at which man might be translated. Other observations made under full-scale test conditions used dogs to assess the hazards of secondary missiles in houses and in open areas[2] and to evaluate the effects of overpressure and displacement inside protective shelters with open entryways.[3,4]

The model dealt with in the present study describes the motion of a missile up to the time of maximum velocity, i.e., when the missile velocity is the same as that of the wind. For some applications a more sophisticated model might be desired which would take into account surface-friction forces during both accelerative and decelerative phases of displacement as well as the decelerative wind forces that occur after maximum velocity has been reached. Such a model would have application to large objects in situations where lofting is not likely to occur. Since total displacement, not displacement at maximum velocity, might be predicted, a model could be used to interpret field data where only total displacement was measured; i.e., total displacement along with appropriate blast data might be sufficient to reconstruct the velocity-time history of the object. It is important to note that this technique need not require a prior knowledge of the object's presented area, mass, or drag coefficient.

Again, it must be pointed out that the missile model described here applies to an ideal or classical blast wave. However, it is well known that blast waves may be modified during their passage through a building or into a structure[3–6] and by the properties of the terrain over which they pass.[1,7,8] Thus, atypical or nonclassical wave forms can and do exist. The important point is that empirical data are at hand for missiles energized by such wave forms. Construction of a theoretical model to predict the behavior of displaced objects under such circumstances can and should be carried out using the experimental data available as a check on the analytical procedures.

Such a model could supplement the present study of blast displacement of objects and allow extension of such thinking to aid in the estimation of missile and displacement damage to man somewhat along the lines of a recent study,[9] which tentatively set forth estimated maximal ranges for human hazards from missiles and displacement wherein the explosive yields were 1 and 10 Mt from an explosive source detonated at the surface of the earth at sea level.

REFERENCES

1. I. Gerald Bowen et al., Secondary Missiles Generated by Nuclear-Produced Blast Waves, Operation Plumbbob Report, WT-1468 (in preparation).
2. V. C. Goldizen, D. R. Richmond, and T. L. Chiffelle, Missile Studies with a Biological Target, Operation Plumbbob Report, WT-1470, January 1961.
3. D. R. Richmond et al., Blast Biology—A Study of the Primary and Tertiary Effects of Blast in Open Underground Protective Shelters, Operation Plumbbob Report, WT-1467, June 30, 1959.
4. C. S. White et al., The Biological Effects of Pressure Phenomena Occurring Inside Protective Shelters Following a Nuclear Detonation, Operation Teapot Report, WT-1179, October 1956.
5. B. B. Dunne and Benedict Cassen, Behavior of Shock Waves Entering Model Bomb Shelters, Report UCLA-332, University of California at Los Angeles, April 1955.
6. Russell E. Duff and Robert N. Hollyer, Jr., The Diffraction of Shock Waves Through Obstacles with Various Openings in Their Front and Back Surfaces, Report 50-3, University of Michigan, Nov. 7, 1950.
7. R. Hetherington, Notes on a Steady Solution of the Refraction of a Blast Wave by a Region of Preheated Air, FWE/62, pp. 23-36, Gt. Brit. Armament Research and Development Establishment, July 25, 1958.
8. A. B. Willoughby, K. Kaplan, and N. R. Wallace, Blast Shielding in Complexes, Report AFSWC-TR-57-29, Broadview Research Corporation, August 1958.
9. C. S. White, Biological Blast Effects, presented before the Special Subcommittee on Radiation of the Joint Committee on Atomic Energy During Public Hearings on The Biological and Environmental Effects of Nuclear War, Washington, D. C., June 24, 1959, Report TID-5564.

Appendix A

APPROXIMATION METHODS TO SUPPLEMENT THE COMPUTED RESULTS

A.1 GENERAL REMARKS

The approximation methods previously described required lengthy computations for numerical solution, although the accuracy attained was satisfactory for a wide range of values of acceleration coefficient. It was realized that other approximation methods could be devised which would require little computational effort but that these methods would be valid only for special conditions, i.e., for short times after the arrival of the blast wave and for very large or for very small acceleration coefficients. Results of these approximations would serve a twofold purpose, that of extending and that of checking the computed results presented in Table 4.1. Material presented in this appendix describes the steps taken to accomplish this purpose.

A.2 EQUATIONS OF MOTION APPLYING FOR SHORT TIMES AFTER ARRIVAL OF THE BLAST WAVE

For short periods after the arrival of the blast wave, the acceleration an object experiences may be considered to be constant. Implicit in the above statement is the assumption that the blast wind and dynamic pressure do not decay and that missile velocity is small compared to both the wind and shock velocities. Thus, stated mathematically in numeric form

$$\frac{dV}{dZ} \equiv \dot{V} = Q_s A \qquad \text{(A.1)}$$

which, upon integration from zero to Z time and from zero to V velocity gives

$$V = Q_s AZ = \frac{dD}{dZ} \qquad \text{(A.2)}$$

Integrating again between the same time values and between zero and D distance

$$D = Q_s AZ^2/2 \qquad \text{(A.3)}$$

If Eqs. A.2 and A.3 are combined to eliminate Z, the following is obtained

$$V^2 = 2Q_s AD \qquad \text{(A.4)}$$

Q_s was evaluated for $P_s = 1.7$ using the equation presented in Sec. 2.3.2, and Eq. A.4 was used to compute V as a function of D for A values of 0.1 and 30. The relations between V and D thus computed are shown graphically in Figure A.1 as dashed straight lines labeled A = 0.1 and A = 30. The curved solid lines that approach tangentially the above mentioned straight lines

were drawn from the computed data presented in Table 4.1. It is interesting to note that at T = 0.03, the approximation is still fairly good for the case where A = 0.1 in contrast to that for A = 30 at the same time T.

A.3 EQUATIONS OF MOTION FOR OBJECTS WITH SMALL ACCELERATION COEFFICIENTS

If an object's acceleration coefficient is sufficiently small, it can be assumed that the velocity attained in a blast situation will be small compared to the wind and shock velocities. Thus, Eq. 2.7 reduces to

$$\frac{dV}{dZ} \equiv \dot{V} = AQ \tag{A.5}$$

Using zero as the initial value of time and velocity, the above expression can be integrated to give

$$V = A \int_0^Z Q\, dZ = \frac{dD}{dZ} \tag{A.6}$$

Equation A.6 can be integrated similarly to give

$$D = A \int_0^Z \int_0^Z Q\, dZ\, dZ \tag{A.7}$$

Combining Eqs. A.6 and A.7 to eliminate A, the following is obtained

$$\frac{V}{D} = \frac{\int_0^Z Q\, dZ}{\int_0^Z \int_0^Z Q\, dZ\, dZ} \tag{A.8}$$

The evaluation of the above integrals can be accomplished by use of Eq. 2.16

$$\int_0^Z Q\, dZ = Q_s\left[\left(\frac{J}{\gamma} e^{-\gamma Z} + \frac{K}{\delta} e^{-\delta Z}\right)(Z-1) + \frac{J}{\gamma^2} e^{-\gamma Z} + \frac{K}{\delta^2} e^{-\delta Z} + \left(\frac{J}{\gamma} + \frac{K}{\delta} - \frac{J}{\gamma^2} - \frac{K}{\delta^2}\right)\right] \tag{A.9}$$

and

$$\begin{aligned}\int_0^Z \int_0^Z Q\, dZ\, dZ = Q_s\Bigg[&-\left(\frac{J}{\gamma^2} e^{-\gamma Z} + \frac{K}{\delta^2} e^{-\delta Z}\right)(Z-1) \\ &- \left(\frac{2J}{\gamma^3} e^{-\alpha Z} + \frac{2K}{\delta^3} e^{-\delta Z}\right) + \left(\frac{J}{\gamma} + \frac{K}{\delta} - \frac{J}{\gamma^2} - \frac{K}{\delta^2}\right) Z \\ &- \left(\frac{J}{\gamma^2} + \frac{K}{\delta^2} - \frac{2J}{\gamma^3} - \frac{2K}{\delta^3}\right)\Bigg]\end{aligned} \tag{A.10}$$

The relations derived above were used to describe V as a function of D for a 1.7-atm blast wave. These solutions are shown in Fig. A.1 as dashed straight lines for T values of 0.03,

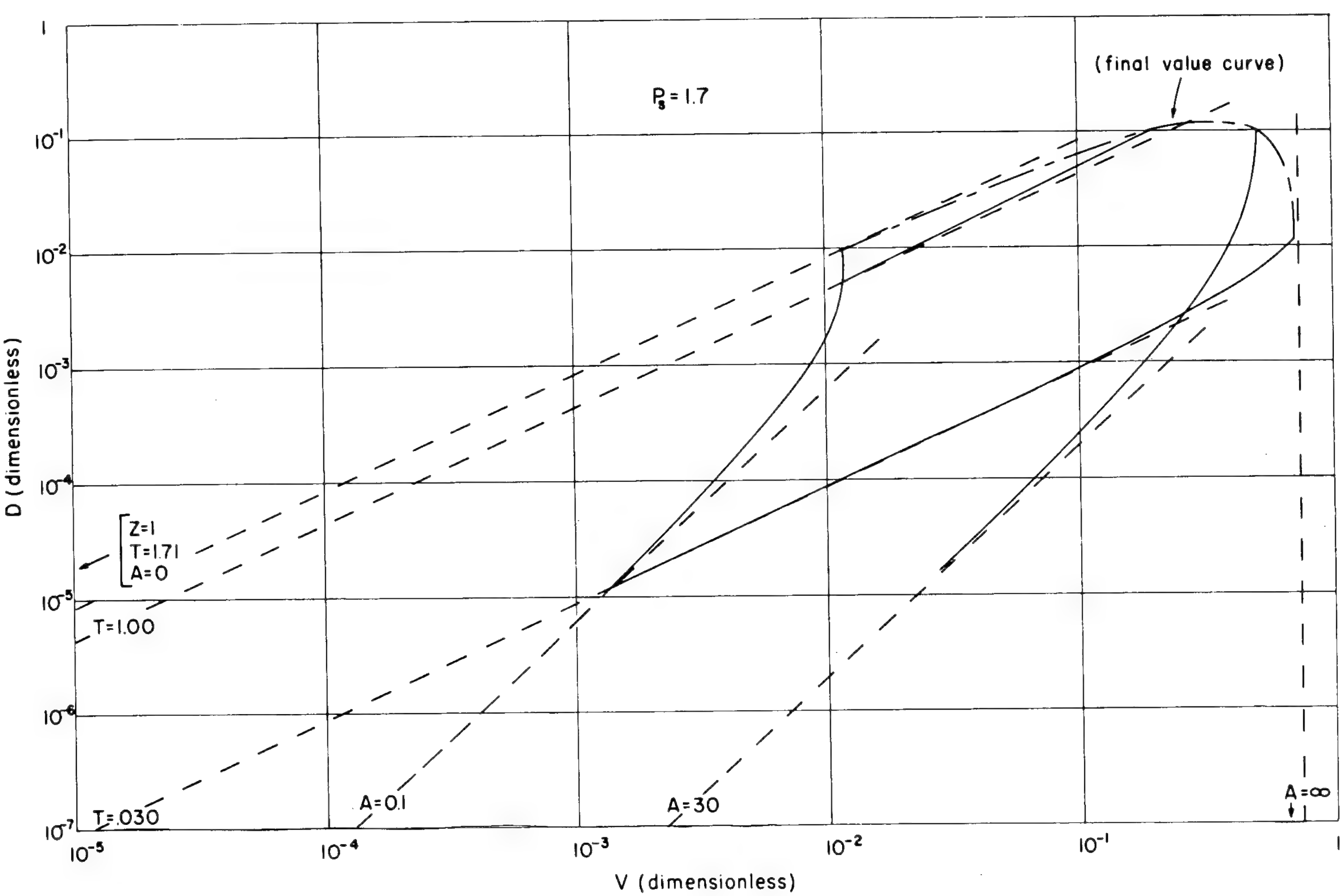

Fig. A.1—Relation between velocity, displacement, and time after arrival of the blast wave (1.7-atm shock overpressure) computed for several values of acceleration coefficient. The solid curves represent accurately computed data, and the dashed lines represent the data derived from approximation methods developed in the appendix. The solid curves were not extrapolated beyond the data presented in Table 4.1.

1.00, and 1.71. For comparative purposes the accurately computed data from Table 4.1 were used to plot the solid curves, which deviate from the approximation lines at the higher values of V and D. It should be noted that for this blast wave ($P_s = 1.7$), $T = 1.71$ corresponds to $Z = 1.0$, i.e., it is assumed for this approximation that the missile was influenced by the entire positive phase of the blast wave. This, clearly, is the limiting case since it requires that the velocity gained by zero and thus $A = 0$. In spite of these assumptions, this approximation (see dashed line for $Z = 1.0$, Fig. A.1) is in fair agreement with the "final-value curve" at $A = 0.1$.

The relation between D_m and A is illustrated in Fig. A.2 for three values of P_s. As in the previous chart, the solid curves were obtained from the accurately computed data and the dashed lines represent approximate relations, which are accurate only for extreme values of A. Equation A.7, with limits on Z from zero to 1, was used to compute the approximation lines for small values of A. The upper approximation lines appearing on this chart are discussed in the next section.

A.4 APPROXIMATION RELATIONS FOR LARGE ACCELERATION COEFFICIENTS

It was found by trial that, for missiles with large acceleration coefficients, it was sufficient to consider the maximum missile velocity equal to the peak wind velocity; however, to estimate missile displacement at maximum velocity, it was necessary to compute by approximation methods missile velocity as a function of time and to take into account the decay of the wind with time.

Wind as a function of time can be approximated (for short times) by a straight-line function, thus

$$U(t) = U_s - BZ \tag{A.11}$$

where B represents the initial slope of the wind-time curve, being a parameter dependent only on P_s.

Using the basic equation, Eq. 2.7, and the approximation written above, the following is obtained

$$dV = Q_s A \left(\frac{U_s - BZ - V}{U_s}\right)^2 \frac{\dot{X}_s}{\dot{X}_s - U_s}\, dZ \tag{A.12}$$

In the above equation, Q was approximated by Q_s; U by U_s, except when V is subtracted from U; and V by U_s for the time-expansion term.

To aid in the solution of the above equation, a new variable is defined, $S = -(U_s - BZ - V)$, whose derivative is $dS = dV + B\,dZ$. After appropriate substitutions, Eq. A.12 becomes

$$\frac{dS}{dZ} = \frac{AQ}{U_s^2} \frac{\dot{X}_s}{\dot{X}_s - U_s} S^2 + B \tag{A.13}$$

Since it is desired to integrate from $V = 0$ when $Z = 0$ to $V = U$ when $Z = Z_m$, the corresponding limits were determined for S as follows (see Eq. A.11): $S = -U_s$ when $Z = 0$ and $S = 0$ when $Z = Z_m$. Thus, application of these limits to the integrated form of Eq. A.13 yields

$$Z_m = \frac{U_s}{\sqrt{AQ_s B \dfrac{\dot{X}_s}{\dot{X}_s - U_s}}} \tan^{-1} \sqrt{\frac{AQ_s}{B} \frac{\dot{X}_s}{\dot{X}_s - U_s}} \tag{A.14}$$

The arc tan factor in the above equation approaches $\pi/2$ as A becomes large.

The initial slope of the wind-time relation (Eq. 2.17) was found to be

$$B = U_s (\nu + 1) \tag{A.15}$$

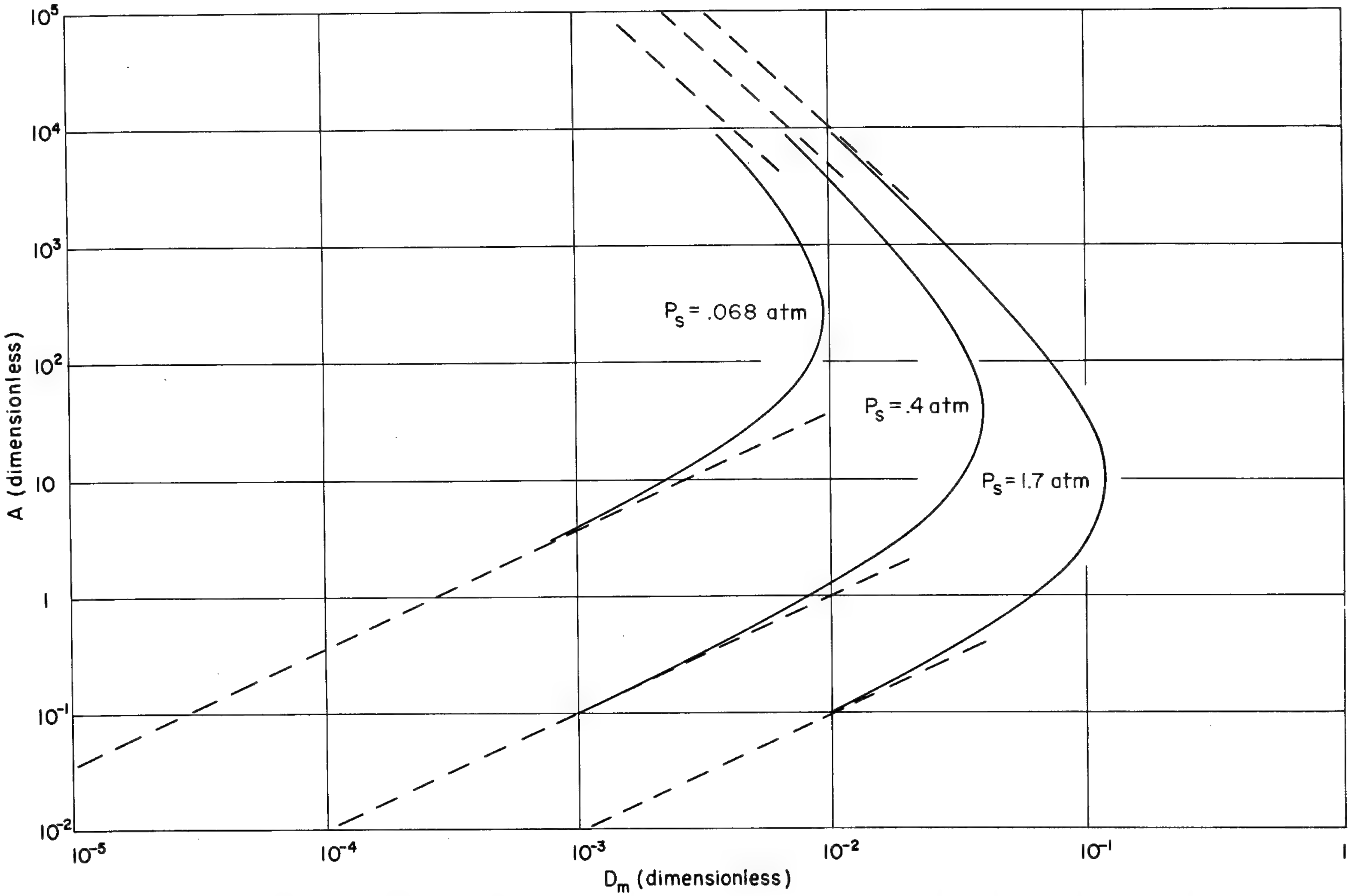

Fig. A.2—Displacement at maximum velocity as a function of acceleration coefficient for various values of shock overpressure. The solid curves represent accurately computed data, and the dashed lines represent the data derived from approximation methods developed in the appendix. The solid curves were not extrapolated beyond the data presented in Table 4.1.

The distance traveled by a missile in reaching maximum velocity is approximately the product of V_m ($\approx U_s$) and the expanded time (see Sec. 2.2.2) required to reach this velocity.

$$D_m = U_s Z_m \frac{\dot{X}_s}{\dot{X}_s - U_s} \tag{A.16}$$

Substituting Eqs. A.14 (with the evaluation of the arc tan function indicated above) and A.15 into Eq. A.16 yields

$$D_m = \frac{\pi}{2} U_s \sqrt{\frac{U_s}{AQ_s(\nu+1)} \frac{\dot{X}_s}{\dot{X}_s - U_s}} \tag{A.17}$$

where ν is defined as function of P_s by Eq. 2.17.

Equation A.17 was used to plot the approximation lines for large values of A appearing in Fig. A.2. It is of interest to note that for a given value of A (10^4, for instance) the approximation of D_m is better for strong blast waves ($P_s = 1.7$) than for weak ones ($P_s = 0.068$). This is probably because in the strong blast wave the missile gains a higher percentage of the peak wind velocity than in the case of the weaker wave.

A.5 NORMALIZED VELOCITY VS. DISTANCE FOR MISSILES WITH LOW ACCELERATION COEFFICIENTS

A relation that has proved useful is normalized velocity (V/V_m) as a function of normalized distance (D/D_m). Computed data from Table 4.1 were used to prepare the plots shown in Fig. A.3 for three values of A for $P_s = 0.068$ (1 psi at sea level). These plots illustrate that the smaller the value of A, the slower is the increase in normalized velocity with increase in normalized distance. Hidden in this relation is the fact that, for a given blast wave, missiles with the smaller values of A are accelerated over longer times and thus longer distances in relation to their velocities. Nevertheless, it would be interesting to determine if there is a limiting curve of V/V_m vs. D/D_m for missiles with A values approaching zero. To accomplish this, Eqs. A.6 and A.7 were used in the following manner (remembering that the maximum velocity and corresponding displacement are reached at a time, Z, approaching unity if the value of A approaches zero):

$$\frac{V}{V_m} = \frac{\int_0^Z Q\,dZ}{\int_0^1 Q\,dZ} \tag{A.18a}$$

and

$$\frac{D}{D_m} = \frac{\int_0^Z \int_0^Z Q\,dZ\,dZ}{\int_0^1 \int_0^Z Q\,dZ\,dZ} \tag{A.18b}$$

The above equations were solved for several corresponding Z values, and the results were used to plot the curve of A = 0 in Fig. A.3.

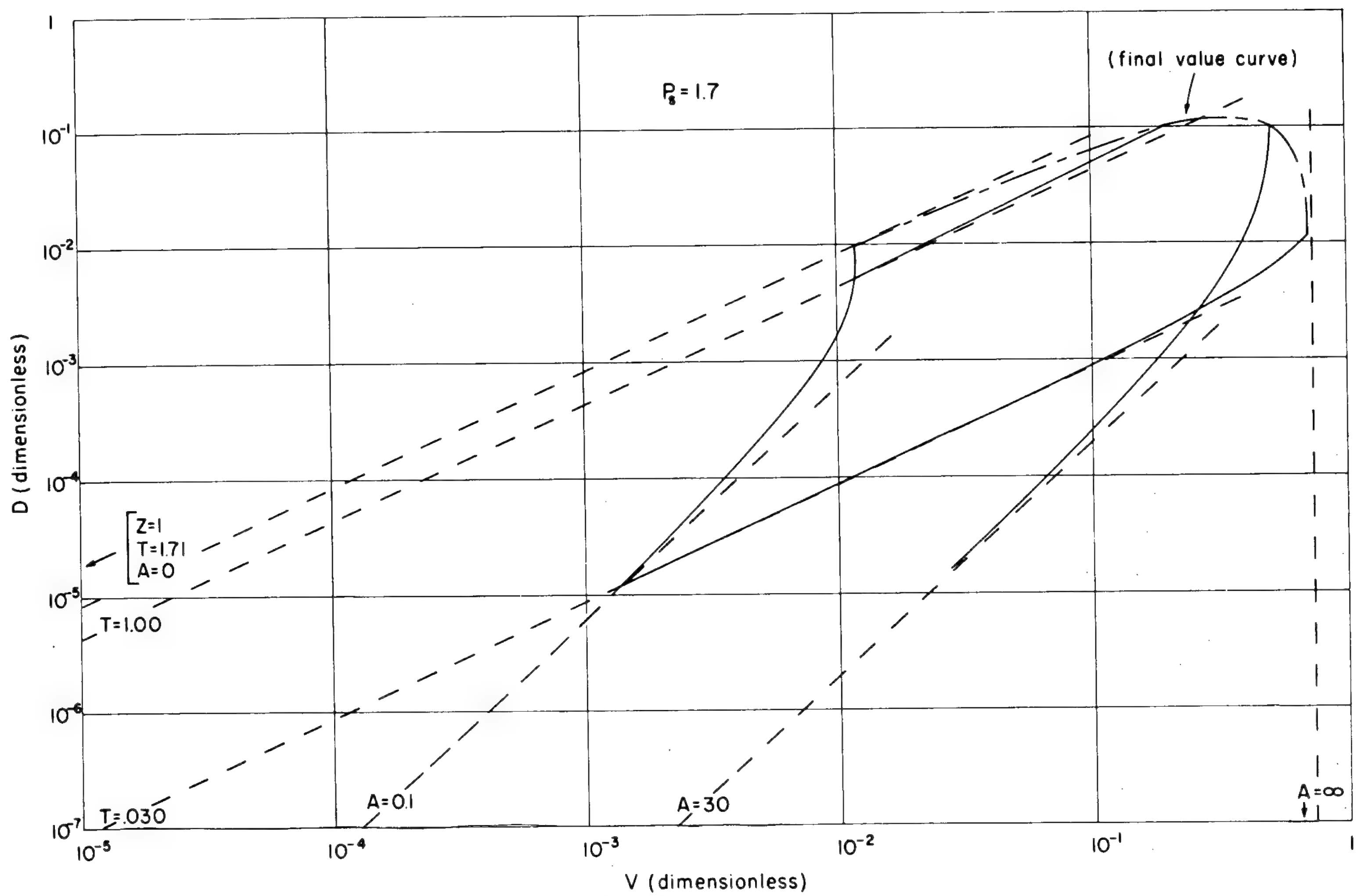

Fig. A.1—Relation between velocity, displacement, and time after arrival of the blast wave (1.7-atm shock overpressure) computed for several values of acceleration coefficient. The solid curves represent accurately computed data, and the dashed lines represent the data derived from approximation methods developed in the appendix. The solid curves were not extrapolated beyond the data presented in Table 4.1.

1.00, and 1.71. For comparative purposes the accurately computed data from Table 4.1 were used to plot the solid curves, which deviate from the approximation lines at the higher values of V and D. It should be noted that for this blast wave ($P_s = 1.7$), $T = 1.71$ corresponds to $Z = 1.0$, i.e., it is assumed for this approximation that the missile was influenced by the entire positive phase of the blast wave. This, clearly, is the limiting case since it requires that the velocity gained by zero and thus $A = 0$. In spite of these assumptions, this approximation (see dashed line for $Z = 1.0$, Fig. A.1) is in fair agreement with the "final-value curve" at $A = 0.1$.

The relation between D_m and A is illustrated in Fig. A.2 for three values of P_s. As in the previous chart, the solid curves were obtained from the accurately computed data and the dashed lines represent approximate relations, which are accurate only for extreme values of A. Equation A.7, with limits on Z from zero to 1, was used to compute the approximation lines for small values of A. The upper approximation lines appearing on this chart are discussed in the next section.

A.4 APPROXIMATION RELATIONS FOR LARGE ACCELERATION COEFFICIENTS

It was found by trial that, for missiles with large acceleration coefficients, it was sufficient to consider the maximum missile velocity equal to the peak wind velocity; however, to estimate missile displacement at maximum velocity, it was necessary to compute by approximation methods missile velocity as a function of time and to take into account the decay of the wind with time.

Wind as a function of time can be approximated (for short times) by a straight-line function, thus

$$U(t) = U_s - BZ \tag{A.11}$$

where B represents the initial slope of the wind-time curve, being a parameter dependent only on P_s.

Using the basic equation, Eq. 2.7, and the approximation written above, the following is obtained

$$dV = Q_s A \left(\frac{U_s - BZ - V}{U_s}\right)^2 \frac{\dot{X}_s}{\dot{X}_s - U_s}\, dZ \tag{A.12}$$

In the above equation, Q was approximated by Q_s; U by U_s, except when V is subtracted from U; and V by U_s for the time-expansion term.

To aid in the solution of the above equation, a new variable is defined, $S = -(U_s - BZ - V)$, whose derivative is $dS = dV + B\,dZ$. After appropriate substitutions, Eq. A.12 becomes

$$\frac{dS}{dZ} = \frac{AQ}{U_s^2} \frac{\dot{X}_s}{\dot{X}_s - U_s} S^2 + B \tag{A.13}$$

Since it is desired to integrate from $V = 0$ when $Z = 0$ to $V = U$ when $Z = Z_m$, the corresponding limits were determined for S as follows (see Eq. A.11): $S = -U_s$ when $Z = 0$ and $S = 0$ when $Z = Z_m$. Thus, application of these limits to the integrated form of Eq. A.13 yields

$$Z_m = \frac{U_s}{\sqrt{AQ_s B \dfrac{\dot{X}_s}{\dot{X}_s - U_s}}} \tan^{-1} \sqrt{\frac{AQ_s}{B} \frac{\dot{X}_s}{\dot{X}_s - U_s}} \tag{A.14}$$

The arc tan factor in the above equation approaches $\pi/2$ as A becomes large.

The initial slope of the wind-time relation (Eq. 2.17) was found to be

$$B = U_s (\nu + 1) \tag{A.15}$$

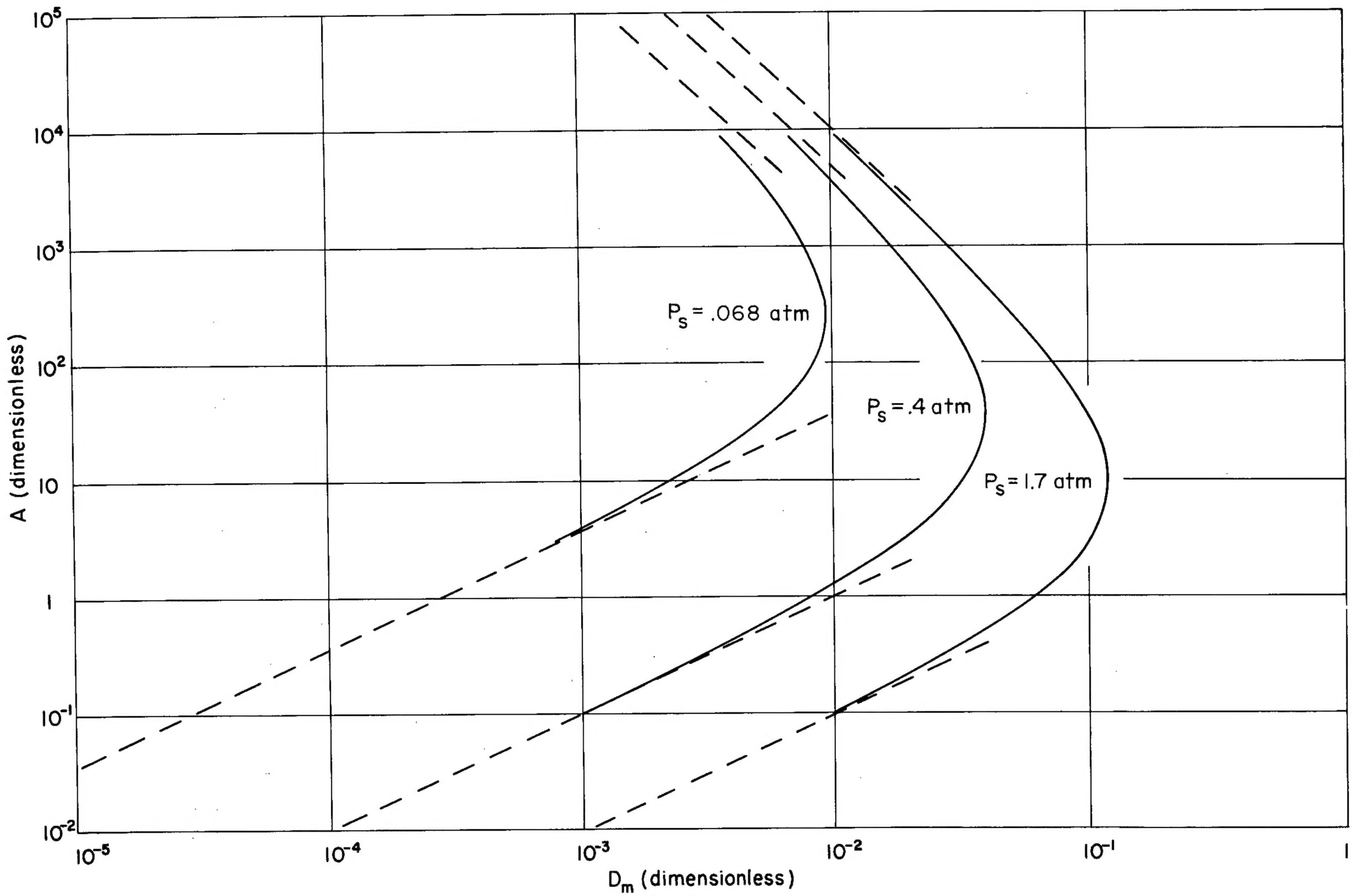

Fig. A.2—Displacement at maximum velocity as a function of acceleration coefficient for various values of shock overpressure. The solid curves represent accurately computed data, and the dashed lines represent the data derived from approximation methods developed in the appendix. The solid curves were not extrapolated beyond the data presented in Table 4.1.

The distance traveled by a missile in reaching maximum velocity is approximately the product of V_m ($\approx U_s$) and the expanded time (see Sec. 2.2.2) required to reach this velocity.

$$D_m = U_s Z_m \frac{\dot{X}_s}{\dot{X}_s - U_s} \tag{A.16}$$

Substituting Eqs. A.14 (with the evaluation of the arc tan function indicated above) and A.15 into Eq. A.16 yields

$$D_m = \frac{\pi}{2} U_s \sqrt{\frac{U_s}{AQ_s(\nu + 1)} \frac{\dot{X}_s}{\dot{X}_s - U_s}} \tag{A.17}$$

where ν is defined as function of P_s by Eq. 2.17.

Equation A.17 was used to plot the approximation lines for large values of A appearing in Fig. A.2. It is of interest to note that for a given value of A (10^4, for instance) the approximation of D_m is better for strong blast waves ($P_s = 1.7$) than for weak ones ($P_s = 0.068$). This is probably because in the strong blast wave the missile gains a higher percentage of the peak wind velocity than in the case of the weaker wave.

A.5 NORMALIZED VELOCITY VS. DISTANCE FOR MISSILES WITH LOW ACCELERATION COEFFICIENTS

A relation that has proved useful is normalized velocity (V/V_m) as a function of normalized distance (D/D_m). Computed data from Table 4.1 were used to prepare the plots shown in Fig. A.3 for three values of A for $P_s = 0.068$ (1 psi at sea level). These plots illustrate that the smaller the value of A, the slower is the increase in normalized velocity with increase in normalized distance. Hidden in this relation is the fact that, for a given blast wave, missiles with the smaller values of A are accelerated over longer times and thus longer distances in relation to their velocities. Nevertheless, it would be interesting to determine if there is a limiting curve of V/V_m vs. D/D_m for missiles with A values approaching zero. To accomplish this, Eqs. A.6 and A.7 were used in the following manner (remembering that the maximum velocity and corresponding displacement are reached at a time, Z, approaching unity if the value of A approaches zero):

$$\frac{V}{V_m} = \frac{\int_0^Z Q\,dZ}{\int_0^1 Q\,dZ} \tag{A.18a}$$

and

$$\frac{D}{D_m} = \frac{\int_0^Z \int_0^Z Q\,dZ\,dZ}{\int_0^1 \int_0^Z Q\,dZ\,dZ} \tag{A.18b}$$

The above equations were solved for several corresponding Z values, and the results were used to plot the curve of A = 0 in Fig. A.3.

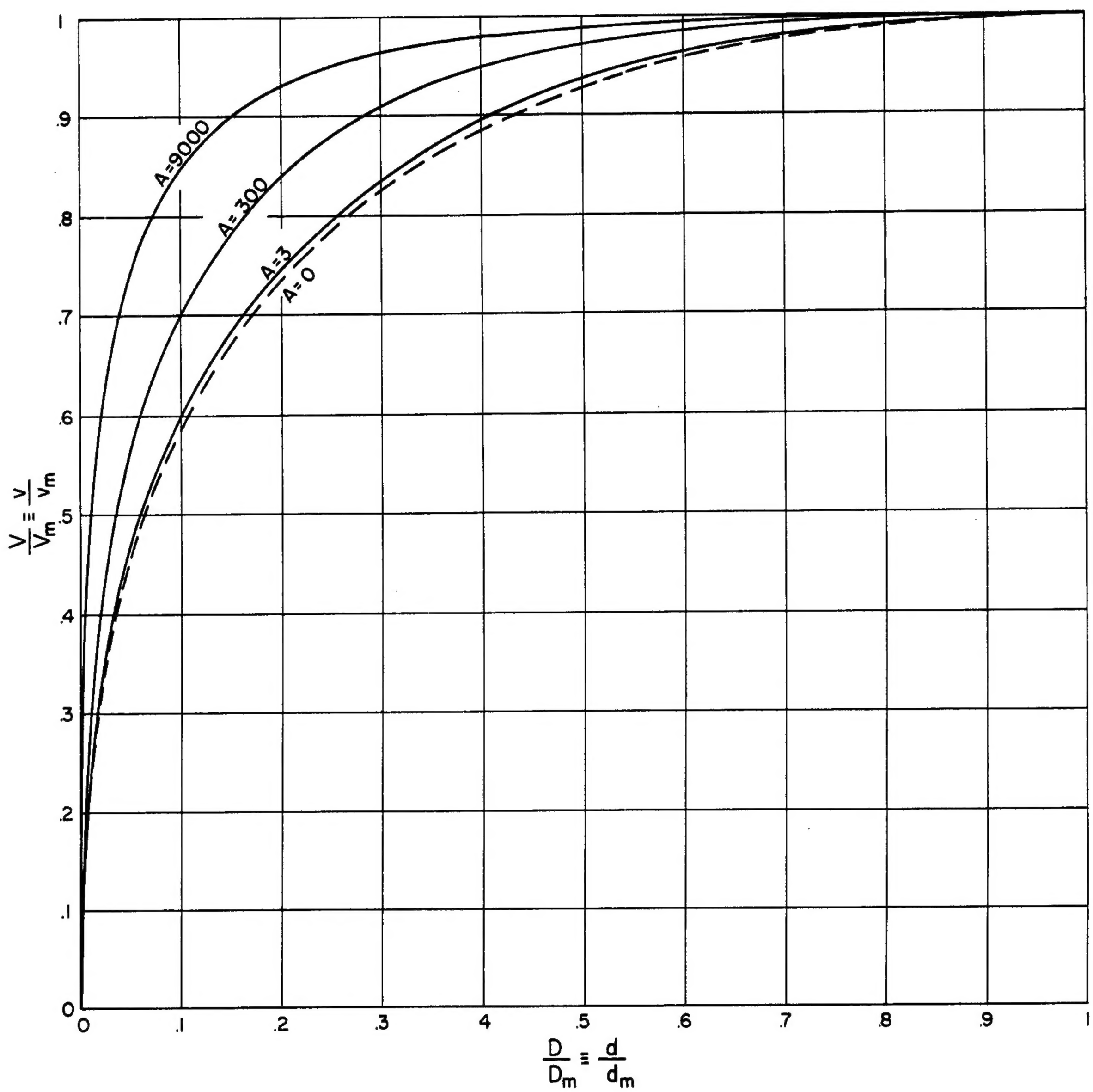

Fig. A.3—Normalized velocity vs. normalized displacement for various values of acceleration coefficient computed for a shock overpressure of 0.068 atm. Data for the solid curves were obtained from Table 4.1, and those for the dashed curve (A = 0) were obtained from approximation methods (see Sec. A.5).

CIVIL EFFECTS TEST OPERATIONS REPORT SERIES (CEX)

Through its Division of Biology and Medicine and Civil Effects Test Operations Office, the Atomic Energy Commission conducts certain technical tests, exercises, surveys, and research directed primarily toward practical applications of nuclear effects information and toward encouraging better technical, professional, and public understanding and utilization of the vast body of facts useful in the design of countermeasures against weapons effects. The activities carried out in these studies do not require nuclear detonations.

A complete listing of all the studies now underway is impossible in the space available here. However, the following is a list of all reports available from studies that have been completed. All reports listed are available from the Office of Technical Services, Department of Commerce, Washington 25, D. C., at the prices indicated.

CEX-57.1 ($0.75) — The Radiological Assessment and Recovery of Contaminated Areas, Carl F. Miller, September 1960.

CEX-58.1 ($2.75) — Experimental Evaluation of the Radiation Protection Afforded by Residential Structures Against Distributed Sources, J. A. Auxier, J. O. Buchanan, C. Eisenhauer, and H. E. Menker, January 1959.

CEX-58.2 ($0.75) — The Scattering of Thermal Radiation into Open Underground Shelters, T. P. Davis, N. D. Miller, T. S. Ely, J. A. Basso, and H. E. Pearse, October 1959.

CEX-58.7 ($0.50) — AEC Group Shelter, AEC Facilities Division, Holmes & Narver, Inc., June 1960.

CEX-58.8 ($1.00) — Comparative Nuclear Effects of Biomedical Interest, Clayton S. White, I. Gerald Bowen, Donald R. Richmond, and Robert L. Corsbie, January 1961.

CEX-59.1 ($0.60) — An Experimental Evaluation of the Radiation Protection Afforded by a Large Modern Concrete Office Building, J. F. Batter, Jr., A. L. Kaplan, and E. T. Clarke, January 1960.

CEX-59.4 ($1.25) — Aerial Radiological Monitoring System. I. Theoretical Analysis, Design, and Operation of a Revised System, R. F. Merian, J. G. Lackey, and J. E. Hand, February 1961.

CEX-59.13 ($0.50) — Experimental Evaluation of the Radiation Protection Afforded by Typical Oak Ridge Homes Against Distributed Sources, T. D. Strickler and J. A. Auxier, April 1960.